

# Leveraging Priors via Diffusion Bridge for Time Series Generation

Jinseong Park<sup>1\*</sup>, Seungyun Lee<sup>1\*</sup>, Woojin Jeong<sup>1</sup>, Yujin Choi<sup>1</sup>, Jaewook Lee<sup>1 †</sup>

<sup>1</sup>Seoul National University  
 {jinseong, rats96, jwj7955, uznhigh, jaewook}@snu.ac.kr

## Abstract

Time series generation is widely used in real-world applications such as simulation, data augmentation, and hypothesis test techniques. Recently, diffusion models have emerged as the de facto approach for time series generation, emphasizing diverse synthesis scenarios based on historical or correlated time series data streams. Since time series have unique characteristics, such as fixed time order and data scaling, standard Gaussian prior might be ill-suited for general time series generation. In this paper, we exploit the usage of diverse prior distributions for synthesis. Then, we propose *TimeBridge*, a framework that enables flexible synthesis by leveraging diffusion bridges to learn the transport between chosen prior and data distributions. Our model covers a wide range of scenarios in time series diffusion models, which leverages (i) data- and time-dependent priors for unconditional synthesis, and (ii) data-scale preserving synthesis with a constraint as a prior for conditional generation. Experimentally, our model achieves state-of-the-art performance in both unconditional and conditional time series generation tasks.

## Introduction

Synthetic time series have expanded their applications by serving roles in data augmentation (Wen et al. 2021), privacy-preserving synthesis (Wang et al. 2024), continuous data compression (Zhou et al. 2023), and simulation of specific hypothesis (Xia et al. 2024) for the data streams. With the advancement of deep generative architectures, time series generative models have been actively investigated such as variational autoencoders (VAE) (Desai et al. 2021; Naiman et al. 2024), generative adversarial networks (GANs) (Yoon, Jarrett, and Van der Schaar 2019; Jeon et al. 2022; Xia et al. 2024), and diffusion models (Ho, Jain, and Abbeel 2020; Karras et al. 2022).

Diffusion models are well-known for producing high-quality and diverse time series data samples (Tashiro et al. 2021; Alcaraz and Strodthoff 2023). The effectiveness of these models relies on iteratively estimating small steps of the reverse trajectory, which corresponds to the forward process towards standard Gaussian priors (Song et al. 2021).

However, modeling diffusion with constraints is not flexible due to the predetermined mapping from noise to data

\*These authors contributed equally.

†Corresponding author.

Preprint.

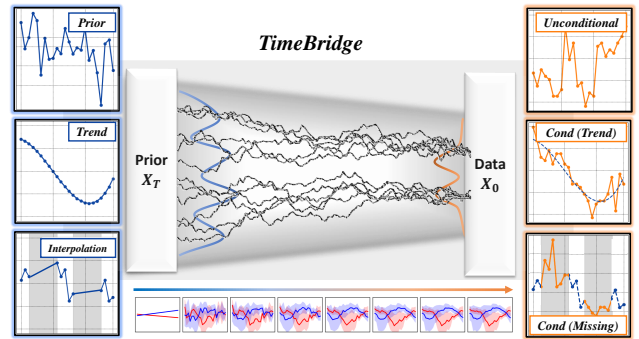


Figure 1: Illustration of the proposed time series diffusion bridge framework focusing on prior design for diverse tasks.

(Harvey et al. 2022; Du et al. 2023). In the time series domain, Coletta et al. (2024) highlighted that generating data under specific bull or bear market patterns requires tailored embedding or penalty functions for sampling guidance. Additionally, the sequential order and data scales (Kim et al. 2022) must be considered when modeling the statistics of historical data and time dependencies (Zeng et al. 2023).

Recently, altering standard Gaussian noise in diffusion models has been explored by modeling the data-dependent distribution in both forward and reverse processes (Han, Zheng, and Zhou 2022; Yu et al. 2024). Specifically, in the time series domain, the noising process should consider not only the diffusion time steps but also the time stamps of temporal data to maintain the continuity of generated data and time dependency (Biloš et al. 2023; Chen et al. 2023a). In this paper, we adopt the diffusion bridge (Schrödinger 1932; De Bortoli et al. 2021; Zhou et al. 2024) to utilize diverse diffusion priors. By learning the optimal transport between the data distribution and fixed priors, diffusion bridges make use of fixed priors and have proven effective in conditional tasks such as image-to-image translation (Li et al. 2023) and text-to-speech synthesis (Chen et al. 2023b).

To push further, we investigate the various prior designs proper for time series tasks. Then, we propose *TimeBridge*, a flexible time series generation framework that addresses multiple time series synthesis with the prior design of diffusion bridge, as shown in Figure 1. We then deeply investigate various experimental settings from unconditional to condi-

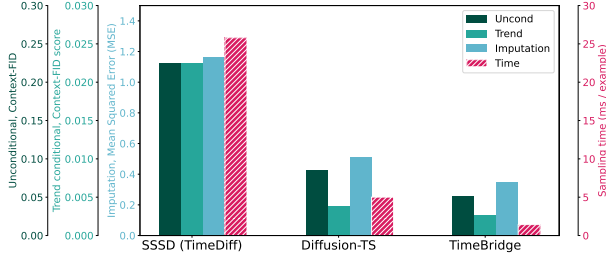


Figure 2: Performance measures (lower is better) on different tasks and sampling time (lower is better) of time series diffusion models. The proposed TimeBridge achieves both generalization in various tasks and sampling efficiency.

tional tasks, achieving state-of-the-art performance across multiple datasets, as illustrated in Figure 2. Our contributions to various situations are summarized as follows:

- We explore the prior selections on time series and propose *TimeBridge*, a diffusion bridge model specifically designed to leverage the priors for time series synthesis.
- For unconditional generation, we propose prior distributions tailored to time series synthesis by leveraging data- and time-dependent properties.
- For conditional generation, we integrate the constraints into the pair-wise prior to maintaining data scales. We also introduce *point-preserving sampling* to preserve constraints, extending its application to imputation tasks.

## Preliminaries

Consider the multivariate time series  $\mathbf{x}$  defined within the sample space  $\mathcal{X} = \mathbb{R}^{d \times \tau}$ , where  $d$  represents the dimensionality of the variables and  $\tau$  denotes the time length. For each index  $i \in \{1, \dots, N\}$  among the  $N$  samples, each time series is denoted as  $\mathbf{x}^i = (\mathbf{x}^i(1), \dots, \mathbf{x}^i(\tau)) \in \mathcal{X}$ , given the data  $\mathbf{x}^i(k) \in \mathbb{R}^d$  for each time step  $k \in \{1, \dots, \tau\}$ . For diffusion steps  $t \in \{0, \dots, T\}$ , we denote intermediate time series samples as  $\mathbf{x}_t$ , and for a specific instance  $i$  as  $\mathbf{x}_t^i$ .

**Diffusion process.** In standard diffusion models (Ho, Jain, and Abbeel 2020), the diffusion process is constructed by gradually injecting noise into samples  $\mathbf{x}_0$  drawn from the data distribution  $p_0$ , forwarding them into a standard Gaussian distribution  $p_T = \mathcal{N}(\mathbf{0}, \mathbf{I})$ . The corresponding stochastic differential equation (SDE) (Song et al. 2021) is:

$$d\mathbf{x}_t = \mathbf{f}(\mathbf{x}_t, t)dt + g(t)d\mathbf{w}_t, \quad (1)$$

where  $\mathbf{f} : \mathbb{R}^d \times [0, T] \rightarrow \mathbb{R}^d$  represents the drift function,  $g : [0, T] \rightarrow \mathbb{R}$  denotes the diffusion coefficient, and  $\mathbf{w}_t$  is the Wiener process. The reverse SDE is formulated as follows:

$$d\mathbf{x}_t = [\mathbf{f}(\mathbf{x}_t, t) - g(t)^2 \nabla_{\mathbf{x}_t} \log p(\mathbf{x}_t)]dt + g(t)d\bar{\mathbf{w}}_t, \quad (2)$$

where  $p(\mathbf{x}_t)$  refers to the probability density of  $\mathbf{x}_t$  (Anderson 1982) and  $\nabla_{\mathbf{x}_t} \log p(\mathbf{x}_t)$  is a score function to match.

**Diffusion bridge.** The aforementioned standard diffusion models cannot be extended to more general tasks due to their inflexibility in choosing a prior distribution. Instead, to construct the diffusion process towards any endpoint, Doob’s h-transform (Doob and Doob 1984) can be applied to Equation (1). With a fixed endpoint  $\mathbf{y}$ , the forward process is:

$$d\mathbf{x}_t = [\mathbf{f}(\mathbf{x}_t, t) + g(t)^2 \mathbf{h}(\mathbf{x}_t, t, \mathbf{y}, T)]dt + g(t)d\mathbf{w}_t, \quad (3)$$

$$\mathbf{x}_0 \sim q_{data}(\mathbf{x}), \mathbf{x}_T = \mathbf{y},$$

where  $\mathbf{h}(\mathbf{x}, t, \mathbf{y}, T) = \nabla_{\mathbf{x}_t} \log p(\mathbf{x}_T | \mathbf{x}_t)|_{\mathbf{x}_t=\mathbf{x}, \mathbf{x}_T=\mathbf{y}}$ . For a given data distribution  $q_{data}(\mathbf{x}, \mathbf{y})$ , the diffusion bridge (Schrödinger 1932; De Bortoli et al. 2021) aims to transport  $\mathbf{x}_0$  to  $\mathbf{x}_T$  where  $(\mathbf{x}_0, \mathbf{x}_T) = (\mathbf{x}, \mathbf{y}) \sim q_{data}(\mathbf{x}, \mathbf{y})$  while following above forward process. Similar to the standard diffusion model, we can construct the reverse SDE as follows:

$$d\mathbf{x}_t = [\mathbf{f}(\mathbf{x}_t, t) - g(t)^2 (\mathbf{s}(\mathbf{x}_t, t, \mathbf{y}, T) - \mathbf{h}(\mathbf{x}_t, t, \mathbf{y}, T))]dt + g(t)d\bar{\mathbf{w}}_t, \quad (4)$$

where  $\mathbf{x}_T = \mathbf{y}$  and its score function is calculated as

$$\mathbf{s}(\mathbf{x}, t, \mathbf{y}, T) = \nabla_{\mathbf{x}_t} \log q(\mathbf{x}_t | \mathbf{x}_T)|_{\mathbf{x}_t=\mathbf{x}, \mathbf{x}_T=\mathbf{y}}. \quad (5)$$

For training, it is sufficient to learn the score  $\mathbf{s}(\mathbf{x}, t, \mathbf{y}, T)$ .

The Schrödinger bridge (Schrödinger 1932) is a closely related concept, focusing on the path optimizations between two arbitrary distributions. Diffusion bridge models have become popular due to their abilities (i) to flexibly map in various domains, including image-to-image translation (Li et al. 2023; Shi et al. 2022) and text-to-speech synthesis (Popov et al. 2021; Chen et al. 2023b), and (ii) to achieve efficient sampling with fewer diffusion steps (Zhou et al. 2024; Chen et al. 2023b).

**Reparametrization of diffusion bridge.** To approximate the score  $\mathbf{s}(\mathbf{x}, t, \mathbf{y}, T)$  in Equation (5), Zhou et al. (2024) recently proposed a Denoising Diffusion Bridge Model (DDBM), integrating the diffusion bridge model in the framework of standard diffusion models. DDBM enables tractable marginal sampling of  $\mathbf{x}_t$ , by designing  $\mathbf{x}_t = \alpha_t \mathbf{x}_0 + \sigma_t \boldsymbol{\varepsilon}$ , where  $\alpha_t$  and  $\sigma_t$  are the noise schedule functions and  $\boldsymbol{\varepsilon} \sim \mathcal{N}(\mathbf{0}, \mathbf{I})$ . For the variance-preserving (VP) schedule, the marginal distribution at time  $t$  is as follows:

$$q(\mathbf{x}_t | \mathbf{x}_0, \mathbf{x}_T) = \mathcal{N}(\hat{\boldsymbol{\mu}}_t, \hat{\sigma}_t^2 \mathbf{I}), \quad (6)$$

$$\hat{\boldsymbol{\mu}}_t = \frac{SNR_T}{SNR_t} \frac{\alpha_t}{\alpha_T} \mathbf{x}_T + \alpha_t \mathbf{x}_0 \left(1 - \frac{SNR_T}{SNR_t}\right), \quad (7)$$

$$\hat{\sigma}_t^2 = \sigma_t^2 \left(1 - \frac{SNR_T}{SNR_t}\right), \quad (8)$$

where signal-to-ratio (SNR) is defined as  $SNR_t = \alpha_t^2 / \sigma_t^2$ . Since the mean  $\hat{\boldsymbol{\mu}}_t$  is a linear combination of  $\mathbf{x}_0$  and  $\mathbf{x}_T$  at time  $t$ , the data scale is preserved for translation. With the reparametrization of Elucidating Diffusion Models (EDM) (Karras et al. 2022), we can match the score as follows:

$$\nabla_{\mathbf{x}_t} \log q(\mathbf{x}_t | \mathbf{x}_T) \approx \mathbf{s}(D_\theta, \mathbf{x}_t, t, \mathbf{x}_T, T)$$

$$:= \frac{\mathbf{x}_t - \left(\frac{SNR_T}{SNR_t} \frac{\alpha_t}{\alpha_T} \mathbf{x}_T + \alpha_t D_\theta(\mathbf{x}_t, t, \mathbf{x}_T)\right) \left(1 - \frac{SNR_T}{SNR_t}\right)}{\sigma_t^2 \left(1 - \frac{SNR_T}{SNR_t}\right)}, \quad (9)$$

where  $D_\theta(\mathbf{x}_t, t, \mathbf{x}_T)$  is the model output as a denoiser.

## Problem Statement

In this section, we cover two types of time series synthesis tasks, i.e., unconditional and conditional generations.

**Unconditional generation** considers the total dataset containing  $N$  samples, denoted as  $\mathcal{D} = \{\mathbf{x}^i\}_{i=1}^N$ . Our goal is to train a deep generative model to mimic the input dataset and yield synthetic samples statistically similar to a given time series dataset. We aim to make the distribution  $p(\hat{\mathbf{x}}|\cdot)$  of synthetic data  $\hat{\mathbf{x}}$ , similar to the input data distribution  $p(\mathbf{x})$ .

**Conditional generation** further utilizes the paired condition  $\mathbf{y}$  to guide time series generation of each data sample  $\mathbf{x}$  as  $\mathcal{D} = \{(\mathbf{x}^i, \mathbf{y}^i)\}_{i=1}^N$ . Thus, we try to make the conditional distribution  $p(\hat{\mathbf{x}}|\mathbf{y})$  of synthetic data  $\hat{\mathbf{x}}$  closely mirror the conditional distribution of input data  $p(\mathbf{x}|\mathbf{y})$ . Considering that the condition in time series is often also a time series as  $\mathbf{y} \in \mathcal{X}$ , Coletta et al. (2024) divided the constraints into two types: (i) **soft constraint** to guide the time series generation such as trend, or (ii) **hard constraint** where we should follow during synthesis such as fixed points. In a broader view, well-known time series tasks can be considered as conditional generation, e.g., the unmasked part in imputation or the historical data of forecasting as conditions.

With the diffusion bridge framework, we hypothesize that the standard Gaussian prior might not be the optimal choice. Thus, we investigate a general time series synthesis framework by analyzing the prior selection in diffusion models based on the following **research questions (RQs)**:

**RQ1.** *Are data-dependent priors effective for time series?*

**RQ2.** *How to model temporal dynamics with priors?*

**RQ3.** *Can constraints be used as priors for diffusion?*

**RQ4.** *How to preserve data points with diffusion bridge?*

### Diffusion Prior Design with TimeBridge

To address these questions, we first explore suitable prior designs for diffusion synthesis. Afterward, we propose *TimeBridge*, a general diffusion bridge model that leverages the aforementioned prior selections, elaborating its application in both unconditional and conditional tasks.

### Data- and Time-dependent Priors for Time Series

For unconditional tasks, we examine the benefit of better priors depending on data and temporal properties of time series.

**Data-Dependent Prior.** To investigate **RQ1**, we suggest using data prior to having a data-dependent distribution to better approximate the data distribution. Sampling from  $\mathcal{N}(\mathbf{0}, \mathbf{I})$  lacks data-specific information, which can be enhanced by enforcing that the priors capture data scale and temporal dependencies. Recently, the usages of data-dependent prior have been investigated for audio (Popov et al. 2021; Lee et al. 2022) and image (Yu et al. 2024) domains. Therefore, we test the use of data-dependent prior for time series by setting the prior distribution as follows:

$$\mathbf{x}_T \sim \mathcal{N}(\boldsymbol{\mu}, \text{diag}(\boldsymbol{\sigma}^2)), \quad (10)$$

where  $\boldsymbol{\mu}$  and  $\boldsymbol{\sigma}^2$  are independently calculated in the same dimension of the time series  $\mathbf{x}$  in  $\mathbb{R}^{\tau \times d}$ .  $\text{diag}(\boldsymbol{\sigma}^2)$  indicates the diagonal covariance matrix of each element.

**Time-Dependent Prior.** As a response to **RQ2**, we focus on capturing temporal dependencies in noise addition towards prior distribution. Recently, Biloš et al. (2023) injected stochastic processes instead of random noise to preserve the continuity of temporal data and Han, Zheng, and Zhou (2022) utilized the pre-trained model for prediction and set the mean of prior as the output for regression.

As a solution, we employ Gaussian processes (GPs) for prior selection, which is effective for modeling temporal data (Biloš et al. 2023; Ansari et al. 2024). GPs are distributions over functions with time input  $k$  characterized by the mean function  $\mathbf{m}(k)$  and the positive definite kernel  $\mathcal{K}(k, k')$ . We use the radial basis function (RBF) kernel, defined as  $\mathcal{K}(k, k') = \eta \exp(-\gamma|k - k'|^2)$ , to ensure a stationary process. To construct a time-dependent prior based on data-dependent properties, we add a variance term to the kernel function to encode data information into the prior distribution. Consequently, we construct the prior incorporating of the temporal dynamics as follows:

$$\mathbf{x}_T \sim \mathcal{GP}(\mathbf{m}, \mathcal{K} + \boldsymbol{\Sigma}), \quad (11)$$

where  $\boldsymbol{\Sigma} = [\boldsymbol{\Sigma}_{ij}]$  is a correlation matrix function in which  $\boldsymbol{\Sigma}_{ij}$  represents the correlation of the data between timestamps  $i$  and  $j$ . For simplified version of Equation (10), we set  $\mathbf{m}$  as  $\boldsymbol{\mu}$  and  $\boldsymbol{\Sigma}$  as  $\text{diag}(\boldsymbol{\sigma}^2)$  to align with the data-dependent prior, i.e.,  $\mathbf{x}_T \sim \mathcal{N}(\boldsymbol{\mu}, \mathcal{K} + \text{diag}(\boldsymbol{\sigma}^2))$ .

### Scale-preserving Sampling for Conditional Priors

We now consider the condition  $\mathbf{y} \in \mathcal{X}$ , provided as a time series, which is the most prevalent case for real-world settings. For example, a given trend can guide the synthesis output or fixed points at specific time steps can determine the properties of synthetic data. We explore the use of a prior on the same data scale instead of relying solely on conditional embedding in standard diffusion.

**Soft constraints with given trends.** To answer **RQ3**, we argue that the diffusion bridge is well-suited for preserving a given condition by setting the prior as the condition. The diffusion bridge has shown its effectiveness in conditional tasks such as coloring (Zhou et al. 2024), image-to-image translation (Li et al. 2023; Liu et al. 2023), and improving naive base predictions (Chen et al. 2023b; Lee et al. 2024).

Conditional generation based on trend is straightforward by (i) setting the pair-wise condition to prior  $\mathbf{x}_T = \mathbf{y}$  and (ii) training the translation from trend to data. As the expected mean of  $\mathbf{x}_t$  is a linear combination of  $\mathbf{x}_0$  and  $\mathbf{x}_T = \mathbf{y}$  in Equation (6), the model learns the correction starting from the trend samples, utilizing the same data scale. In contrast, standard diffusion models are unsuitable for translating conditions into synthetic data; instead, they generate new data based on a specific trend condition, typically requiring additional steps such as providing guidance or correcting intermediate data samples  $\mathbf{x}_t$  during sampling. Thus, we can also eliminate the need for additional penalty functions or value correction during sampling.

**Hard constraints with fixed points.** In **RQ4**, preserving data points of hard constraints can be important in conditional tasks. To ensure the fixed point condition during

sampling, we introduce a novel *point-preserving sampling* method that prevents adding noise to the values to be fixed. This is a unique trait of our framework because standard diffusion models cannot preserve identity trajectories to the constrained values from Gaussian noise. We make details of the proposed sampling method in Appendix .

The direct case of fixed point constraints is imputation. With the mask  $\mathbf{m}$  indicating the missing value as 0, we construct the condition  $\mathbf{c} = \mathbf{y} \odot \mathbf{m}$  for imputation. However, unlike soft constraints that apply to all values in  $\mathbf{y} \in \mathbb{R}^{\tau \times d}$ , the condition for imputation  $\mathbf{c} \in \mathbb{R}^{\tau \times d}$  has missing values, which should be interpolated to data-dependent values rather than zeros. Therefore, we build local linear models for condition-to-time series imputation. We adopt *linear spline interpolation* (De Boor 1978) to generate a prior for fixed point constraints. In a feature-wise manner, let us consider  $x \in \mathbb{R}$  to be a single dimensional input of  $\mathbf{x} \in \mathbb{R}^d$ . With a set  $K$  of feature-wise observed times for  $x$ , the prior  $x_T$  with the interpolation of each feature with timestamp  $k$  is:

$$x_T(k) = x(k_{j-1}) + \frac{x(k_j) - x(k_{j-1})}{k_j - k_{j-1}}(k - k_{j-1}), \quad (12)$$

$$k_{j-1} \leq k < k_j, \quad j = 1, \dots, |K| - 1.$$

Note that before the first observation,  $k < k_0$ ,  $x_T(k) = x(k_0)$ . After the last observation,  $k \geq k_{|K|-1}$ ,  $x_T(k) = x(k_{|K|-1})$ . The detailed Algorithm is in Appendix .

### TimeBridge: Bridge Modeling for Time Series

Based on the aforementioned prior selections, we propose *TimeBridge*, a general diffusion bridge model for time series synthesis. Our approach yields high-quality samples with fewer sampling steps and is compatible with existing time series diffusion frameworks.

For score matching in Equation (9), we build the denoiser  $D_\theta$  for time series. For architecture design, we adopt the backbone of Diffusion-TS (Yuan and Qiao 2024), i.e., Fourier-based loss function (Zhou et al. 2022; Liu et al. 2024; Nguyen et al. 2022; Yi et al. 2024) and transformer encoder-decoder models with seasonal-trend decomposition (Zeng et al. 2023; Wu et al. 2021). With the bridge diffusion framework, our objective function is formulated as follows:

$$\mathcal{L}_\theta = \mathbb{E}_{t, \mathbf{x}_0} [w_t (\|\mathbf{x}_0 - D_\theta(\mathbf{x}_t, t, \mathbf{x}_T)\|^2 + \lambda \|FFT(\mathbf{x}_0) - FFT(D_\theta(\mathbf{x}_t, t, \mathbf{x}_T))\|^2)]. \quad (13)$$

$w_t$  indicates the weight scheduler of the loss function and  $\lambda$  indicates the strength of fast Fourier transform (FFT). We construct the bridge model to produce output by decomposing the input into trend and seasonal components as follows:

$$D_\theta = V_t^{tr}(\theta, \mathbf{x}_t, t, \mathbf{x}_T) + \sum_{i=1}^K S_{i,t}(\theta, \mathbf{x}_t, t, \mathbf{x}_T) + R(\theta, \mathbf{x}_t, t, \mathbf{x}_T), \quad (14)$$

where  $V_t^{tr}$  is the output for the trend synthesis layer,  $S_{i,t}$  is the output for each seasonal synthesis layer  $i$  among  $K$  layers and  $R$  is the output for estimated residual.

As time series data possess stochasticity (Shen and Kwok 2023), we directly predict  $D_\theta$  rather than using parametrization technique from noise prediction used in other domains

(Karras et al. 2022; Zhou et al. 2024). Moreover, we utilize the second-order Heun sampler (Ascher and Petzold 1998; Karras et al. 2022), achieving both quality and efficiency. Overall, our TimeBridge model leverages the flexibility of prior selection as a diffusion bridge designed for time series.

## Related Works

**Standard diffusion models for time series.** Time series diffusion models have become the de facto method in synthesis tasks. Rasul et al. (2021) initially used diffusion networks for time series based on recurrent networks. For imputation, SSSD (Alcaraz and Strodthoff 2023) and CSDI (Tashiro et al. 2021) considered time series imputation similar to image inpainting tasks. TimeDiff (Shen and Kwok 2023), LDT (Feng et al. 2024), and TMDM (Li et al. 2024) focused on time series forecasting tasks. Recently, Coletta et al. (2024) investigated guiding the sampling with a penalty function called DiffTime. Diffusion-TS (Yuan and Qiao 2024) introduced a decomposition architecture to disentangle time series data into trend and seasonal components and applied a Fourier-based loss term. They also expanded their unconditional model to conditional generation tasks by guiding the diffusion sampling toward the input conditions.

**Existing time series bridge models.** Recently, some researchers have investigated the use of the diffusion bridge in the time series domain. Chen et al. (2023a) investigated the convergence analysis of the Schrödinger bridge algorithm and applied them to time series imputation tasks. Hamdouche, Henry-Labordere, and Pham (2023) used kernel estimation for the Schrödinger bridge combined with feed-forward and LSTM networks, especially for the application of deep hedging on real-data sets. Garg, Zhang, and Zhou (2024) relaxed the Schrödinger bridge by setting a geometric mixture of targets and other distributions for the prior distribution and applied their method to time series. However, most of them used iterative solutions for bridge problems, which required a heavy computational burden and incompatibility with recent standard diffusion models. Furthermore, none of them suggested a general framework for both unconditional and conditional time series generation.

## Experiments

### Experimental Setup

We assess the performance of TimeBridge using widely used time series datasets. We use two simulation datasets: **Sines** with 5 features of different frequencies and phases of sine functions and **MuJoCo** of multivariate advanced physics simulation with 14 features. For real-world datasets, we use **ETT** (Electricity Transformer Temperature) for long-term electric power with 7 features, **Stocks** of Google stock prices and volumes with 6 features, **Energy**, UCI dataset with appliances energy use in a low energy building with 28 features, and **fMRI** of the blood oxygen level-dependent functional MR imaging with 50 selected features.

For measures, we assess four metrics for unconditional time series generation on a normalized (0-1) scale. Context-Fréchet Inception Distance (Context-FID) score (Jeha et al.

Metric	Methods	Synthetic datasets		Real datasets				Average (rank)
		Sines	MuJoCo	ETTh	Stocks	Energy	fMRI	
Context-FID score (Lower is better)	TimeVAE <sup>†</sup>	0.307±.060	0.251±.015	0.805±.186	0.215±.035	1.631±.142	14.449±.969	2.943 (8)
	TimeGAN <sup>†</sup>	0.101±.014	0.563±.052	0.300±.013	0.103±.013	0.767±.103	1.292±.218	0.521 (6)
	Cot-GAN <sup>†</sup>	1.337±.068	1.094±.079	0.980±.071	0.408±.086	1.039±.028	7.813±.550	2.112 (7)
	Diffwave <sup>†</sup>	0.014±.002	0.393±.041	0.873±.061	0.232±.032	1.031±.131	0.244±.018	0.465 (5)
	DiffTime <sup>†</sup>	<b>0.006±.001</b>	0.188±.028	0.299±.044	0.236±.074	0.279±.045	0.340±.015	0.225 (4)
	Diffusion-TS	<u>0.008±.001</u>	<b>0.012±.002</b>	0.129±.008	0.165±.043	0.095±.014	0.106±.007	0.086 (3)
	<b>TimeBridge</b>	<u>0.008±.001</u>	0.018±.002	<u>0.069±.004</u>	<u>0.079±.023</u>	<u>0.082±.007</u>	<u>0.097±.008</u>	0.059 (2)
	<b>TimeBridge-GP</b>	<b>0.006±.001</b>	<u>0.016±.002</u>	<b>0.067±.007</b>	<b>0.054±.009</b>	<b>0.064±.007</b>	<b>0.096±.008</b>	<b>0.051 (1)</b>
Correlational score (Lower is better)	TimeVAE <sup>†</sup>	0.131±.010	0.388±.041	0.111±.020	0.095±.008	1.688±.226	17.296±.526	3.285 (6)
	TimeGAN <sup>†</sup>	0.045±.010	0.886±.039	0.210±.006	0.063±.005	4.010±.104	23.502±.039	4.786 (7)
	Cot-GAN <sup>†</sup>	0.049±.010	1.042±.007	0.249±.009	0.087±.004	3.164±.061	26.824±.449	5.236 (8)
	Diffwave <sup>†</sup>	0.022±.005	0.579±.018	0.175±.006	0.030±.020	5.001±.154	3.927±.049	1.622 (5)
	DiffTime <sup>†</sup>	<b>0.017±.004</b>	0.218±.031	0.067±.005	<b>0.006±.002</b>	1.158±.095	1.501±.048	0.495 (4)
	Diffusion-TS	<b>0.017±.006</b>	0.193±.015	0.049±.012	0.011±.008	<b>0.874±.163</b>	1.151±.053	0.383 (3)
	<b>TimeBridge</b>	0.024±.001	0.179±.011	<u>0.035±.005</u>	0.009±.009	1.064±.167	0.914±.028	0.371 (2)
	<b>TimeBridge-GP</b>	<u>0.018±.003</u>	<b>0.173±.025</b>	<b>0.034±.004</b>	<u>0.008±.008</u>	<u>0.902±.218</u>	<b>0.839±.018</b>	<b>0.329 (1)</b>
Discriminative score (Lower is better)	TimeVAE <sup>†</sup>	0.041±.044	0.230±.102	0.209±.058	0.145±.120	0.499±.000	0.476±.044	0.267 (7)
	TimeGAN <sup>†</sup>	0.011±.008	0.238±.068	0.114±.055	0.102±.021	0.236±.012	0.484±.042	0.198 (5)
	Cot-GAN <sup>†</sup>	0.254±.137	0.426±.022	0.325±.099	0.230±.016	0.498±.002	0.492±.018	0.371 (8)
	Diffwave <sup>†</sup>	0.017±.008	0.203±.096	0.190±.008	0.232±.061	0.493±.004	0.402±.029	0.256 (6)
	DiffTime <sup>†</sup>	0.013±.006	0.154±.045	0.100±.007	0.097±.016	0.445±.004	0.245±.051	0.176 (4)
	Diffusion-TS	<u>0.008±.012</u>	0.009±.011	0.074±.010	0.083±.044	<b>0.126±.007</b>	0.133±.024	0.072 (3)
	<b>TimeBridge</b>	0.012±.003	<u>0.007±.008</u>	<b>0.052±.004</b>	<u>0.052±.021</u>	0.167±.003	<b>0.077±.010</b>	0.061 (2)
	<b>TimeBridge-GP</b>	<b>0.002±.002</b>	<b>0.006±.003</b>	<b>0.052±.002</b>	<b>0.049±.014</b>	<u>0.165±.009</u>	<u>0.082±.033</u>	<b>0.059 (1)</b>

The baseline experimental results (denoted by <sup>†</sup>) are adopted from (Yuan and Qiao 2024). We re-implement Diffusion-TS with their official code.

Table 1: Quality comparison of unconditional time series synthetic data. The best results are in **bold** and the second best are underlined. We report the average score (lower is better) and rank of each method.

2022) measures the distributional quality for mean and variance projected on embedding on trained TS2Vec (Yue et al. 2022). Correlational score (Liao et al. 2020) measures temporal dependency of real and synthetic data using the absolute error of cross-correlation. Discriminative score (Yoon, Jarrett, and Van der Schaar 2019) measures the performance of a classifier trained to distinguish original and synthetic data in a supervised manner. Additionally, for imputation tasks, we calculate the mean squared error (MSE) and mean absolute error (MAE) on each data scale.

Our experiments are conducted using PyTorch on four NVIDIA GeForce RTX 4090 GPUs. We report the mean and its interval of five experiments. For the detailed settings, refer to Appendix .

## Unconditional Generation

We demonstrate the unconditional generation tasks with a length of 24 for the aforementioned datasets and evaluate the performance of the previous measures. For baseline methods, we compare with TimeVAE (Desai et al. 2021), TimeGAN (Yoon, Jarrett, and Van der Schaar 2019), Cot-GAN (Xu et al. 2020), Diffwave (Kong et al. 2021), DiffTime (Coletta et al. 2024) with SSSD (Alcaraz and Strodthoff 2023) backbone, and Diffusion-TS (Yuan and Qiao 2024). For the proposed TimeBridge, we choose the data-dependent settings in Equation (10) and TimeBridge-GP denotes the time-dependent GP prior in Equation (11).

Results are shown in Table 1. We observe that the proposed method outperforms the previous methods. The per-

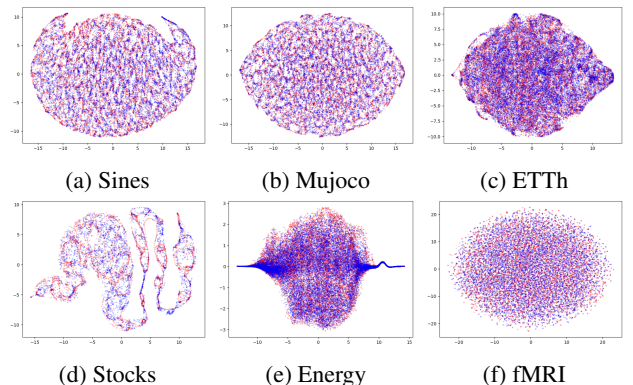


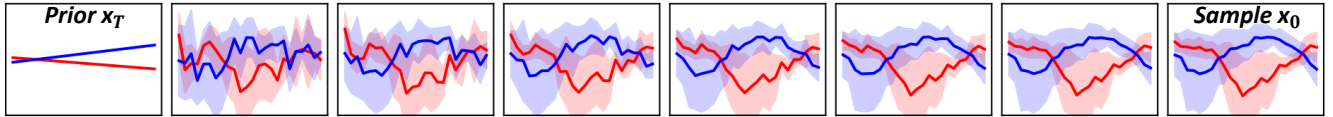
Figure 3: Visualization on t-SNE. Red and blue indicate original and synthetic data, respectively.

formance gain is significant in context-FID and discriminative scores, reducing the scores of 40.70% and 18.05% on average, respectively. Notably, the strength of data and time-dependent prior is shown in real datasets, such as ETTh and Stocks. This indicates that our prior selection and modeling help in approximating the data distribution during synthesis.

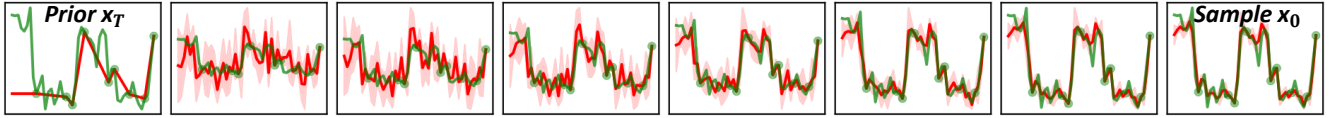
To visualize the generated data, we plot the t-SNE plots with the generated data in Figure 3. The red original data and the blue synthetic data show the overlapped plot in almost all datasets. The generated samples well approximate the distribution properties in complex datasets, such as the Stocks and Energy datasets. For further visualization con-

Metric	Methods	ETTh			Energy			Average (rank)
		Linear	Polynomial	Butterworth	Linear	Polynomial	Butterworth	
Context-FID score	Trend Baseline	0.1729±.0228	0.1000±.0790	0.7343±.6795	0.8343±.0531	0.5864±.2016	0.8093±.2690	0.5395 (-)
	SSSD	0.0137±.0028	0.0281±.0136	0.0575±.0104	0.0146±.0085	0.0135±.0015	0.0075±.0057	0.0225 (3)
	Diffusion-TS	0.0049±.0008	0.0028±.0003	0.0030±.0003	0.0052±.0006	0.0050±.0005	0.0024±.0003	0.0039 (2)
	<b>TimeBridge</b>	<b>0.0028±.0003</b>	<b>0.0024±.0002</b>	<b>0.0023±.0002</b>	<b>0.0031±.0002</b>	<b>0.0036±.0002</b>	<b>0.0017±.0002</b>	<b>0.0027 (1)</b>
Correlation score	Trend Baseline	0.0493±.0104	0.0372±.0139	0.0524±.0194	0.4816±.0633	0.4816±.0999	0.5246±.0915	0.2711 (-)
	SSSD	0.0362±.0137	0.0334±.0074	0.0404±.0032	0.6186±.1124	0.5594±.0925	0.5138±.0917	0.3003 (3)
	Diffusion-TS	0.0247±.0109	<b>0.0238±.0113</b>	0.0239±.0127	0.4834±.2090	0.4843±.2116	<b>0.4816±.2093</b>	0.2536 (2)
	<b>TimeBridge</b>	<b>0.0240±.0120</b>	<b>0.0238±.0124</b>	<b>0.0237±.0123</b>	<b>0.4828±.2101</b>	<b>0.4830±.2106</b>	0.4833±.2071	<b>0.2534 (1)</b>
Discriminative score	Trend Baseline	0.1258±.0795	0.0574±.0626	0.1380±.0943	0.5000±.0633	0.4996±.0004	0.4997±.0003	0.3034 (-)
	SSSD	0.0272±.0105	0.0301±.0142	0.1108±.0915	0.1871±.0749	0.2198±.0385	0.1360±.0797	0.1185 (3)
	Diffusion-TS	0.0045±.0038	0.0038±.0040	0.0043±.0045	<b>0.0031±.0035</b>	0.0067±.0044	0.0046±.0034	0.0045 (2)
	<b>TimeBridge</b>	<b>0.0036±.0038</b>	<b>0.0023±.0021</b>	<b>0.0021±.0022</b>	0.0054±.0026	<b>0.0056±.0048</b>	<b>0.0037±.0035</b>	<b>0.0038 (1)</b>

Table 2: Quality comparison of trend-conditioned time series synthetic data.



(a) Sampling of TimeBridge by applying the two pair-wise linear trends (red/blue) as priors.



(b) Imputation (red) of TimeBridge with point-preserving sampling using observed values (dots) of truth (green).

Figure 4: Illustration of sampling path from (Left) prior to (Right) data samples on the ETTh.

cerning PCA and kernel density plots, refer to Appendix .

### Synthesis with Trend Condition

We now consider trend-guided generation, where the data samples are in  $\mathcal{D} = \{(\mathbf{x}^i, \mathbf{y}^i)\}_{i=1}^N$ . For the trend  $\mathbf{y}$ , we consider three types: linear, polynomial with degree of three, and Butterworth filter (Butterworth et al. 1930), a signal processing filter that captures trends (Xia et al. 2024). Using these trends as conditions, we reimplement the experiments in Table 1 with the ETTh and Energy datasets. To apply the condition to baseline methods, we feed the trend into a conditional embedding and concatenate it with the original embedding. For the proposed TimeBridge, we set the prior  $\mathbf{x}_T = \mathbf{y}$  upon the conditional embedding for translation.

Experimental results are shown in Table 2. The rows with trend baseline indicate the results with the trends without any synthesis. After synthesis with trend conditions, we observe that the quality metrics such as Context-FID, correlation, and discriminative scores diminished compared to the unconditional generation in Table 1, indicating that trend conditions help the model generate more realistic data samples. With the trend condition in  $\mathbf{x}_T$ , the proposed TimeBridge achieves the best performance in Context-FID in all settings and the best discriminative score in 5 out of 6 settings while maintaining correlation scores at similar levels to Diffusion-TS. This indicates that the proposed framework can be broadly adopted by different conditioning settings, without controlling any details other than the prior distribu-

tion. The sampling path of TimeBridge from trend to data is shown in Figure 4a.

### Imputation with Fixed Masks

For imputation, which is a common setting of hard conditions, we compare the proposed method with imputation diffusion models and the conditional Langevin sampler of Diffusion-TS (Yuan and Qiao 2024). We use random masks for the Mujoco dataset and the geometric mask from Zerveas et al. (2021) for the ETTh and Energy datasets, with a given missing ratio as in Yuan and Qiao (2024). We set the total length of imputation to 100 for the Mujoco dataset, matching the data length, and split the ETTh and Energy datasets into 48 time steps. For the proposed TimeBridge, we preserve the observed values and set the prior  $\mathbf{x}_T$  as the interpolated values of the condition  $\mathbf{c}$  as in Equation (12).

The imputation results are shown in Table 3 and Table 4. Both tables demonstrate that TimeBridge achieves the lowest measures in imputation tasks. Since the Langevin sampler of Diffusion-TS does not require individual training for various missing ratios, we ensure a fair comparison by evaluating TimeBridge with the same training setting, TimeBridge-75%, which uses 75% missing values for training. The performance of TimeBridge-75% even outperforms the models trained with equal missing values, highlighting the generalization capability of TimeBridge in imputation tasks. The visualization of imputation results is shown in Figure 5, and the sampling path can be found in Figure 4b.

Methods	RNN GRU-D	ODE -RNN	Neural CDE	Latent -ODE	NAOMI	NRTSI	CSDI	SSSD	Diffusion -TS	<b>TimeBridge</b>
70%	11.34	9.86	8.35	3	1.46	0.63	<u>0.24±.03</u>	0.59±.08	0.37±.03	<b>0.19±.00</b>
80%	14.21	12.09	10.71	2.95	2.32	1.22	0.61±.10	1.00±.05	<u>0.43±.03</u>	<b>0.26±.02</b>
90%	19.68	16.47	13.52	3.6	4.42	4.06	4.84±.02	1.90±.03	<u>0.73±.12</u>	<b>0.60±.02</b>

The baseline experimental results are adopted from (Alcaraz and Strothoff 2023) and (Yuan and Qiao 2024).

Table 3: Imputation results of MSE in the order of  $1e-3$  on the Mujoco dataset with a random mask of ratio  $\{0.7, 0.8, 0.9\}$ . The best results are in **bold** and the second best are underlined.

Metric	Methods	MSE				MAE			
		SSSD	Diffusion-TS	<b>TimeBridge</b>	<b>TimeBridge-75%</b>	SSSD	Diffusion-TS	<b>TimeBridge</b>	<b>TimeBridge-75%</b>
ETTh	25%	0.496±0.049	0.406±0.006	<u>0.159±0.014</u>	<b>0.146±0.007</b>	0.433±0.009	0.378±0.001	<b>0.220±0.001</b>	<b>0.220±0.002</b>
	50%	0.523±0.061	0.561±0.010	0.226±0.010	<b>0.199±0.006</b>	0.435±0.013	0.422±0.001	0.248±0.002	<b>0.237±0.002</b>
	75%	<b>0.588±0.012</b>	0.774±0.006	<u>0.661±0.031</u>	<u>0.661±0.031</u>	0.449±0.001	0.497±0.001	<b>0.366±0.004</b>	<b>0.366±0.004</b>
Energy	25%	108.82±19.12	137.77±1.14	<u>17.06±2.34</u>	<b>12.03±0.40</b>	1.94±0.19	1.39±0.00	<u>0.47±0.01</u>	<b>0.45±0.00</b>
	50%	107.68±29.14	163.86±1.02	<u>30.64±3.00</u>	<b>23.07±2.13</b>	1.77±0.10	1.70±0.01	<u>0.71±0.02</u>	<b>0.63±0.01</b>
	75%	139.07±4.49	199.38±1.82	<b>63.84±2.15</b>	<b>63.84±2.15</b>	1.87±0.01	2.09±0.01	<b>1.07±0.01</b>	<b>1.07±0.01</b>

Table 4: Imputation result of MSE and MAE on the ETTh and Energy datasets with a geometric mask of ratio  $\{0.25, 0.5, 0.75\}$ . The best results are in **bold** and the second best are underlined.

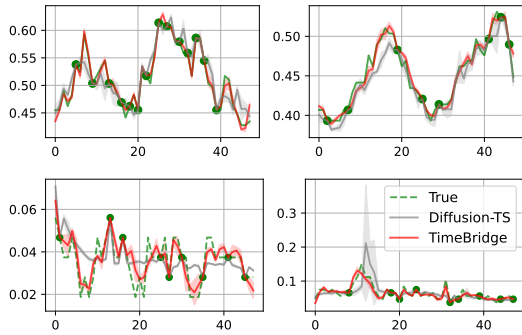


Figure 5: Visualization of imputation on (Top) ETTh and (Bottom) Energy dataset. The green dotted lines and circles denote true and observed value, respectively. Each method is visualized along with their interval.

## Ablation study

Table 5 evaluates the effectiveness of training design with three variants: (1) variance exploding (VE) scheduler, (2) noise matching instead of directly predicting  $D_\theta$  as in Zhou et al. (2024), and (3) without Fourier-based loss during training. Further experimental results of the ablation study are presented in Appendix .

Metric	Methods	Datasets	
		ETTh	Energy
Context-FID score (Lower is better)	TimeBridge-GP	<b>0.067±.007</b>	<b>0.064±.007</b>
	VE scheduler	0.256±.028	0.184±.003
	F-matching	0.087±.010	0.081±.006
	w/o Fourier	0.087±.010	0.093±.011
Discriminative score (Lower is better)	TimeBridge-GP	<b>0.052±.002</b>	<b>0.165±.009</b>
	VE scheduler	0.089±.009	0.236±.012
	F-matching	<b>0.052±.012</b>	0.170±.007
	w/o Fourier	0.060±.004	0.216±.007

Table 5: Ablation study for training and sampling features.

## Computation efficiency

Table 6 illustrates the strength of the proposed method, particularly when using the second-order Heun sampler during sampling. With a lower number of score function evaluations (NFE), our sampler achieves fast synthesis without compromising quality. We use 40 steps for sampling in all experiments, resulting in 119 NFEs with our settings. For comparison, we evaluate the Diffusion-TS using the same NFE. Given the trade-off of performance and sampling time in Diffusion-TS, our experimental results outperform previous methods. The marginal increase in time for TimeBridge is due to the time required to build the prior distribution.

Data	ETTh				Stocks			
	NFE	Time	C.-FID	Disc.	NFE	Time	C.-FID	Disc.
Diffusion-TS	500	5.008	0.129	0.074	500	4.670	0.165	0.083
<b>TimeBridge</b>	119	1.038	0.244	0.103	119	1.104	0.252	0.130

Table 6: Comparison of sampling efficiency and generation performance. The time column indicates the generation time of each sample in milliseconds (ms) with a batch size of 512.

## Conclusion

In this paper, we highlight the effectiveness of selecting prior distributions for time series generation using diffusion bridges. To address the limitations in the standard Gaussian prior of the diffusion models, we propose a framework that allows for the selection of any prior suitable for various tasks. As a limitation, we leave experiments on other types of conditions, such as class labels or time-independent conditions, for future work. We believe that incorporating sampling guidance can address these types of conditions. As the proposed method can cover a wide range of scenarios in time series diffusion models, we believe this work significantly advances the investigation of prior distributions for developing a general time series generation framework.

## References

- Alcaraz, J. L.; and Strodthoff, N. 2023. Diffusion-based Time Series Imputation and Forecasting with Structured State Space Models. *Transactions on Machine Learning Research*.
- Anderson, B. D. 1982. Reverse-time diffusion equation models. *Stochastic Processes and their Applications*, 12(3): 313–326.
- Ansari, A. F.; Stella, L.; Turkmen, C.; Zhang, X.; Mercado, P.; Shen, H.; Shchur, O.; Rangapuram, S. S.; Arango, S. P.; Kapoor, S.; et al. 2024. Chronos: Learning the language of time series. *arXiv preprint arXiv:2403.07815*.
- Ascher, U. M.; and Petzold, L. R. 1998. *Computer methods for ordinary differential equations and differential-algebraic equations*. SIAM.
- Biloš, M.; Rasul, K.; Schneider, A.; Nevmyvaka, Y.; and Günnemann, S. 2023. Modeling temporal data as continuous functions with stochastic process diffusion. In *International Conference on Machine Learning*, 2452–2470. PMLR.
- Butterworth, S.; et al. 1930. On the theory of filter amplifiers. *Wireless Engineer*, 7(6): 536–541.
- Chen, T.; Liu, G.-H.; and Theodorou, E. A. 2021. Likelihood training of schrödinger bridge using forward-backward sdes theory. *arXiv preprint arXiv:2110.11291*.
- Chen, Y.; Deng, W.; Fang, S.; Li, F.; Yang, N. T.; Zhang, Y.; Rasul, K.; Zhe, S.; Schneider, A.; and Nevmyvaka, Y. 2023a. Provably convergent Schrödinger bridge with applications to probabilistic time series imputation. In *International Conference on Machine Learning*, 4485–4513. PMLR.
- Chen, Z.; He, G.; Zheng, K.; Tan, X.; and Zhu, J. 2023b. Schrodinger Bridges Beat Diffusion Models on Text-to-Speech Synthesis.
- Coletta, A.; Gopalakrishnan, S.; Borrajo, D.; and Vyetrenko, S. 2024. On the constrained time-series generation problem. *Advances in Neural Information Processing Systems*, 36.
- De Boor, C. 1978. *A practical guide to splines*, volume 27. Springer New York.
- De Bortoli, V.; Thornton, J.; Heng, J.; and Doucet, A. 2021. Diffusion Schrödinger bridge with applications to score-based generative modeling. *Advances in Neural Information Processing Systems*, 34: 17695–17709.
- Desai, A.; Freeman, C.; Wang, Z.; and Beaver, I. 2021. Timevae: A variational auto-encoder for multivariate time series generation. *arXiv preprint arXiv:2111.08095*.
- Doob, J. L.; and Doob, J. 1984. *Classical potential theory and its probabilistic counterpart*, volume 262. Springer.
- Du, W.; Zhang, H.; Yang, T.; and Du, Y. 2023. A flexible diffusion model. In *International Conference on Machine Learning*, 8678–8696. PMLR.
- Feng, S.; Miao, C.; Zhang, Z.; and Zhao, P. 2024. Latent Diffusion Transformer for Probabilistic Time Series Forecasting. In *Proceedings of the AAAI Conference on Artificial Intelligence*, volume 38, 11979–11987.
- Fortet, R. 1940. Résolution d’un système d’équations de M. Schrödinger. *Journal de Mathématiques Pures et Appliquées*, 19(1-4): 83–105.
- Garg, J.; Zhang, X.; and Zhou, Q. 2024. Soft-constrained Schrödinger Bridge: a Stochastic Control Approach. In *International Conference on Artificial Intelligence and Statistics*, 4429–4437. PMLR.
- Hamdouche, M.; Henry-Labordere, P.; and Pham, H. 2023. Generative modeling for time series via Schrödinger bridge. *arXiv preprint arXiv:2304.05093*.
- Han, X.; Zheng, H.; and Zhou, M. 2022. Card: Classification and regression diffusion models. *Advances in Neural Information Processing Systems*, 35: 18100–18115.
- Harvey, W.; Naderiparizi, S.; Masrani, V.; Weilbach, C.; and Wood, F. 2022. Flexible diffusion modeling of long videos. *Advances in Neural Information Processing Systems*, 35: 27953–27965.
- Ho, J.; Jain, A.; and Abbeel, P. 2020. Denoising diffusion probabilistic models. *Advances in neural information processing systems*, 33: 6840–6851.
- Jeha, P.; Bohlke-Schneider, M.; Mercado, P.; Kapoor, S.; Nirwan, R. S.; Flunkert, V.; Gasthaus, J.; and Januschowski, T. 2022. PSA-GAN: Progressive self attention GANs for synthetic time series. In *The Tenth International Conference on Learning Representations*.
- Jeon, J.; Kim, J.; Song, H.; Cho, S.; and Park, N. 2022. GT-GAN: General purpose time series synthesis with generative adversarial networks. *Advances in Neural Information Processing Systems*, 35: 36999–37010.
- Karras, T.; Aittala, M.; Aila, T.; and Laine, S. 2022. Elucidating the design space of diffusion-based generative models. *Advances in Neural Information Processing Systems*, 35: 26565–26577.
- Kim, T.; Kim, J.; Tae, Y.; Park, C.; Choi, J.-H.; and Choo, J. 2022. Reversible Instance Normalization for Accurate Time-Series Forecasting against Distribution Shift. In *International Conference on Learning Representations*.
- Kong, Z.; Ping, W.; Huang, J.; Zhao, K.; and Catanzaro, B. 2021. DiffWave: A Versatile Diffusion Model for Audio Synthesis. In *International Conference on Learning Representations*.
- Kullback, S. 1968. Probability densities with given marginals. *The Annals of Mathematical Statistics*, 39(4): 1236–1243.
- Lee, D.; Lee, D.; Bang, D.; and Kim, S. 2024. DiSCO: Diffusion Schrödinger Bridge for Molecular Conformer Optimization. In *Proceedings of the AAAI Conference on Artificial Intelligence*, volume 38, 13365–13373.
- Lee, S.; Kim, H.; Shin, C.; Tan, X.; Liu, C.; Meng, Q.; Qin, T.; Chen, W.; Yoon, S.; and Liu, T.-Y. 2022. PriorGrad: Improving Conditional Denoising Diffusion Models with Data-Dependent Adaptive Prior. In *International Conference on Learning Representations*.
- Léonard, C. 2012. From the Schrödinger problem to the Monge–Kantorovich problem. *Journal of Functional Analysis*, 262(4): 1879–1920.
- Li, B.; Xue, K.; Liu, B.; and Lai, Y.-K. 2023. Bbdm: Image-to-image translation with brownian bridge diffusion models. In *Proceedings of the IEEE/CVF conference on computer vision and pattern Recognition*, 1952–1961.

- Li, Y.; Chen, W.; Hu, X.; Chen, B.; baolin sun; and Zhou, M. 2024. Transformer-Modulated Diffusion Models for Probabilistic Multivariate Time Series Forecasting. In *The Twelfth International Conference on Learning Representations*.
- Liao, S.; Ni, H.; Szpruch, L.; Wiese, M.; Sabate-Vidales, M.; and Xiao, B. 2020. Conditional sig-wasserstein gans for time series generation. *arXiv preprint arXiv:2006.05421*.
- Lipman, Y.; Chen, R. T.; Ben-Hamu, H.; Nickel, M.; and Le, M. 2022. Flow matching for generative modeling. *arXiv preprint arXiv:2210.02747*.
- Liu, G.-H.; Vahdat, A.; Huang, D.-A.; Theodorou, E. A.; Nie, W.; and Anandkumar, A. 2023. I2SB: image-to-image Schrödinger bridge. In *Proceedings of the 40th International Conference on Machine Learning*, 22042–22062.
- Liu, Y.; Li, C.; Wang, J.; and Long, M. 2024. Koopa: Learning non-stationary time series dynamics with koopman predictors. *Advances in Neural Information Processing Systems*, 36.
- Naiman, I.; Erichson, N. B.; Ren, P.; Mahoney, M. W.; and Azencot, O. 2024. Generative Modeling of Regular and Irregular Time Series Data via Koopman VAEs. In *The Twelfth International Conference on Learning Representations*.
- Nguyen, T.; Pham, M.; Nguyen, T.; Nguyen, K.; Osher, S.; and Ho, N. 2022. Fourierformer: Transformer meets generalized fourier integral theorem. *Advances in Neural Information Processing Systems*, 35: 29319–29335.
- Popov, V.; Vovk, I.; Gogoryan, V.; Sadekova, T.; and Kudinov, M. 2021. Grad-tts: A diffusion probabilistic model for text-to-speech. In *International Conference on Machine Learning*, 8599–8608. PMLR.
- Rasul, K.; Seward, C.; Schuster, I.; and Vollgraf, R. 2021. Autoregressive denoising diffusion models for multivariate probabilistic time series forecasting. In *International Conference on Machine Learning*, 8857–8868. PMLR.
- Schrödinger, E. 1932. Sur la théorie relativiste de l'électron et l'interprétation de la mécanique quantique. In *Annales de l'institut Henri Poincaré*, volume 2, 269–310.
- Shen, L.; and Kwok, J. 2023. Non-autoregressive conditional diffusion models for time series prediction. In *International Conference on Machine Learning*, 31016–31029. PMLR.
- Shi, Y.; De Bortoli, V.; Campbell, A.; and Doucet, A. 2024. Diffusion Schrödinger bridge matching. *Advances in Neural Information Processing Systems*, 36.
- Shi, Y.; De Bortoli, V.; Deligiannidis, G.; and Doucet, A. 2022. Conditional simulation using diffusion Schrödinger bridges. In *Uncertainty in Artificial Intelligence*, 1792–1802. PMLR.
- Song, J.; Meng, C.; and Ermon, S. 2020. Denoising Diffusion Implicit Models. In *International Conference on Learning Representations*.
- Song, Y.; Sohl-Dickstein, J.; Kingma, D. P.; Kumar, A.; Ermon, S.; and Poole, B. 2021. Score-Based Generative Modeling through Stochastic Differential Equations. In *International Conference on Learning Representations*.
- Tashiro, Y.; Song, J.; Song, Y.; and Ermon, S. 2021. Csd: Conditional score-based diffusion models for probabilistic time series imputation. *Advances in Neural Information Processing Systems*, 34: 24804–24816.
- Vargas, F.; Thodoroff, P.; Lamacraft, A.; and Lawrence, N. 2021. Solving schrödinger bridges via maximum likelihood. *Entropy*, 23(9): 1134.
- Wang, W.; Tang, P.; Lou, J.; Shao, Y.; Waller, L.; Ko, Y.-a.; and Xiong, L. 2024. IGAMT: Privacy-Preserving Electronic Health Record Synthesization with Heterogeneity and Irregularity. In *Proceedings of the AAAI Conference on Artificial Intelligence*, volume 38, 15634–15643.
- Wen, Q.; Sun, L.; Yang, F.; Song, X.; Gao, J.; Wang, X.; and Xu, H. 2021. Time Series Data Augmentation for Deep Learning: A Survey. In *Proceedings of the Thirtieth International Joint Conference on Artificial Intelligence*. International Joint Conferences on Artificial Intelligence Organization.
- Wu, H.; Xu, J.; Wang, J.; and Long, M. 2021. Autoformer: Decomposition transformers with auto-correlation for long-term series forecasting. *Advances in neural information processing systems*, 34: 22419–22430.
- Xia, H.; Sun, S.; Wang, X.; and An, B. 2024. Market-GAN: Adding Control to Financial Market Data Generation with Semantic Context. In *Proceedings of the AAAI Conference on Artificial Intelligence*, volume 38, 15996–16004.
- Xu, T.; Wenliang, L. K.; Munn, M.; and Acciaio, B. 2020. Cot-gan: Generating sequential data via causal optimal transport. *Advances in neural information processing systems*, 33: 8798–8809.
- Yi, K.; Zhang, Q.; Fan, W.; Wang, S.; Wang, P.; He, H.; An, N.; Lian, D.; Cao, L.; and Niu, Z. 2024. Frequency-domain MLPs are more effective learners in time series forecasting. *Advances in Neural Information Processing Systems*, 36.
- Yoon, J.; Jarrett, D.; and Van der Schaar, M. 2019. Time-series generative adversarial networks. *Advances in neural information processing systems*, 32.
- Yu, X.; Gu, X.; Liu, H.; and Sun, J. 2024. Constructing non-isotropic Gaussian diffusion model using isotropic Gaussian diffusion model for image editing. *Advances in Neural Information Processing Systems*, 36.
- Yuan, X.; and Qiao, Y. 2024. Diffusion-TS: Interpretable Diffusion for General Time Series Generation. In *The Twelfth International Conference on Learning Representations*.
- Yue, Z.; Wang, Y.; Duan, J.; Yang, T.; Huang, C.; Tong, Y.; and Xu, B. 2022. Ts2vec: Towards universal representation of time series. In *Proceedings of the AAAI Conference on Artificial Intelligence*, volume 36, 8980–8987.
- Zeng, A.; Chen, M.; Zhang, L.; and Xu, Q. 2023. Are transformers effective for time series forecasting? In *Proceedings of the AAAI conference on artificial intelligence*, volume 37, 11121–11128.
- Zerveas, G.; Jayaraman, S.; Patel, D.; Bhamidipaty, A.; and Eickhoff, C. 2021. A transformer-based framework for multivariate time series representation learning. In *Proceedings*

of the 27th ACM SIGKDD conference on knowledge discovery & data mining, 2114–2124.

Zhou, L.; Lou, A.; Khanna, S.; and Ermon, S. 2024. Denoising Diffusion Bridge Models. In *The Twelfth International Conference on Learning Representations*.

Zhou, L.; Poli, M.; Xu, W.; Massaroli, S.; and Ermon, S. 2023. Deep latent state space models for time-series generation. In *International Conference on Machine Learning*, 42625–42643. PMLR.

Zhou, T.; Ma, Z.; Wen, Q.; Wang, X.; Sun, L.; and Jin, R. 2022. Fedformer: Frequency enhanced decomposed transformer for long-term series forecasting. In *International conference on machine learning*, 27268–27286. PMLR.

## Diffusion Bridge

We introduce the details of the diffusion bridge mathematically, and how this framework is embraced in recent deep learning architectures.

**Schrödinger Bridge.** Standard diffusion models suffer from limitations such as the requirement of a sufficiently long time for the prior distribution to approximate a standard Gaussian distribution and the computational expense associated with sample generation. To address these challenges, diffusion Schrödinger bridge models have been recently introduced (De Bortoli et al. 2021; Chen, Liu, and Theodorou 2021). The goal of the Schrödinger bridge problem is to find an entropic optimal transport between two probability distributions in terms of Kullback–Leibler divergence on path spaces within a finite horizon (Chen, Liu, and Theodorou 2021; Léonard 2012). While standard diffusion models and flow matching models are not guaranteed to provide optimal transport, Schrödinger bridge models aim to find paths that recover entropy-regularized versions of optimal transport (Shi et al. 2024). The formulation of the Schrödinger bridge problem is as follows:

$$\min_{p \in \mathcal{P}_{[0,T]}} D_{KL}(p \| p^{ref}), \quad s.t. p_0 = p_{data}, p_T = p_{prior}, \quad (15)$$

where  $\mathcal{P}_{[0,T]}$  refers to the space of path measures on  $[0, T]$ ,  $p^{ref}$  denotes the reference path measure, and  $p_0, p_T$  represents the marginal distributions of  $p$  at each time step  $0, T$ , respectively. The diffusion bridge algorithm is introduced by utilizing  $p^{ref}$  from the forward SDE in Equation (1) (Vargas et al. 2021; Chen, Liu, and Theodorou 2021; De Bortoli et al. 2021). Setting the reference path as the forward SDE, the problem becomes equivalent to following forward-backward SDEs:

$$d\mathbf{x}_t = [\mathbf{f}(\mathbf{x}_t, t) + g^2(t) \nabla \log \Psi_t(\mathbf{x}_t)] dt + g(t) d\mathbf{w}_t, \quad (16)$$

$\mathbf{x}_0 \sim p_{data},$

$$d\mathbf{x}_t = [\mathbf{f}(\mathbf{x}_t, t) - g^2(t) \nabla \log \hat{\Psi}_t(\mathbf{x}_t)] dt + g(t) d\bar{\mathbf{w}}_t, \quad (17)$$

$\mathbf{x}_T \sim p_{prior},$

where  $\nabla \log \Psi_t(\mathbf{x}_t)$  and  $\nabla \log \hat{\Psi}_t(\mathbf{x}_t)$  are described by following PDEs:

$$\begin{aligned} \frac{\partial \Psi}{\partial t} &= -\nabla_x \Psi^T \mathbf{f} - \frac{1}{2} \text{tr}(g^2 \nabla_x^2 \Psi) \\ \frac{\partial \hat{\Psi}}{\partial t} &= -\nabla_x \cdot (\hat{\Psi} \mathbf{f}) + \frac{1}{2} \text{tr}(g^2 \nabla_x^2 \hat{\Psi}) \\ s.t. \quad \Psi_0 \hat{\Psi}_0 &= p_{data}, \Psi_T \hat{\Psi}_T = p_{prior}, \\ p_t &= \Psi_t \hat{\Psi}_t \text{ for } t \in [0, T]. \end{aligned} \quad (18)$$

The Schrödinger bridge problem can be addressed using iterative methods (Kullback 1968; Fortet 1940). At the outset, several early studies employed iterative methods to simulate trajectories converging to the Schrödinger bridge problem (Vargas et al. 2021; Shi et al. 2024; De Bortoli et al. 2021). However, these methods rely on expensive iterative approximation techniques and have seen limited empirical application (Zhou et al. 2024).

**Denosing Diffusion Bridge Models.** Alternatively, Chen, Liu, and Theodorou (2021) leveraged the theory of forward-backward SDEs to derive an exact log-likelihood expression for the Schrödinger bridge, which accurately generalizes the approach for score generative models. Drawing inspiration from the perspective that the framework of diffusion bridges, employing forward-backward SDEs, encompasses the paradigms of score matching diffusion models (Song, Meng, and Ermon 2020) and flow matching optimal transport paths (Lipman et al. 2022). Zhou et al. (2024) demonstrated that reintroducing several design choices from these domains becomes feasible. In particular, the reparameterization techniques outlined in Karras et al. (2022) are utilized.

For noise scheduling, common options include variance-preserving (VP) and variance-exploding (VE) diffusion (Song, Meng, and Ermon 2020). We express the reparameterization for the VP and VE bridge of Zhou et al. (2024) in Table 7. In our study, we choose to utilize the VP bridge, as our experimental findings indicate its superiority of VP over VE.

For score matching, Karras et al. (2022) proved that if a denoiser function  $D(\mathbf{x}; \sigma)$  minimizes the expected  $L_2$  error for samples drawn from  $p_{data}$ , then  $D(\mathbf{x}; \sigma)$  becomes the linear function of score function, i.e., if  $D(\mathbf{x}; \sigma)$  minimizes  $\mathbb{E}_{\mathbf{y} \sim p_{data}} \mathbb{E}_{\boldsymbol{\varepsilon} \sim \mathcal{N}(\mathbf{0}, \sigma^2 \mathbf{I})} \|D(\mathbf{y} + \boldsymbol{\varepsilon}; \sigma) - \mathbf{y}\|_2^2$ , then  $\nabla_x \log p(\mathbf{x}; \sigma) = (D(\mathbf{x}; \sigma) - \mathbf{x})/\sigma^2$ . Thus, we can train  $D_\theta$  directly instead of training the score function. In general, training a neural network to model  $D_\theta$  directly is ineffective, due to its vast variance, which heavily depends on the noise level. Thus, Karras et al. (2022) reconstructed  $D_\theta$  with  $\sigma$ -dependent skip connection as follows:

$$D_\theta(\mathbf{x}; \sigma) = c_{skip}(\sigma) \mathbf{x} + c_{out}(\sigma) F_\theta(c_{in}(\sigma) \mathbf{x}; c_{noise}(\theta)), \quad (19)$$

and trained  $F_\theta$  instead of  $D_\theta$  with the neural network. However, for time series data, estimating the diffusion noise poses greater challenges due to the presence of highly irregular noisy components (Shen and Kwok 2023; Yuan and Qiao 2024). Consistent with these studies, our experiments demonstrate that  $D$ -matching is more effective than  $F$ -matching. Detailed experimental results for comparison of VP with VE and  $D$ -matching with  $F$ -matching are provided in the ablation study in the Appendix .

## Details of Datasets and Baselines

We first illustrate time series generation situations on various conditions in Figure 6.

**Data explanation.** Table 8 presents the statistics of the datasets along with their online links.

**Baseline methods.** For the unconditional baseline methods, we compare with TimeVAE (Desai et al. 2021), TimeGAN (Yoon, Jarrett, and Van der Schaar 2019), CotGAN (Xu et al. 2020), Diffwave (Kong et al. 2021), Diff-Time (Coletta et al. 2024), and Diffusion-TS (Yuan and Qiao 2024). For Table 1, we note the quality evaluation results in Diffusion-TS. We reimplement Diffusion-TS using their official GitHub in <https://github.com/Y-debug-sys/Diffusion->

	$\mathbf{f}(\mathbf{x}_t, t)$	$g^2(t)$	$p(\mathbf{x}_t   \mathbf{x}_0)$	$SNR_t$	$\nabla_{\mathbf{x}_t} \log p(\mathbf{x}_T   \mathbf{x}_t)$
VP	$\frac{d \log \alpha_t}{dt} \mathbf{x}_t$	$\frac{d}{dt} \sigma_t^2 - 2 \frac{d \log \alpha_t}{dt} \sigma_t^2$	$\mathcal{N}(\alpha_t \mathbf{x}_0, \sigma_t^2 \mathbf{I})$	$\alpha_t^2 / \sigma_t^2$	$\frac{(\alpha_t / \alpha_T) \mathbf{x}_T - \mathbf{x}_t}{\sigma_t^2 (SNR_t / SNR_T - 1)}$
VE	0	$\frac{d}{dt} \sigma_t^2$	$\mathcal{N}(\mathbf{x}_0, \sigma_t^2 \mathbf{I})$	$1 / \sigma_t^2$	$\frac{\mathbf{x}_T - \mathbf{x}_t}{\sigma_T^2 - \sigma_t^2}$

Table 7: VP and VE instantiations of diffusion bridge settings in DDBM.

Table 8: Details of datasets.

Dataset	Sample size	# of features	Link
Sines	10000	5	<a href="https://github.com/jsyoon0823/TimeGAN">https://github.com/jsyoon0823/TimeGAN</a>
Stocks	3773	6	<a href="https://finance.yahoo.com/quote/GOOG">https://finance.yahoo.com/quote/GOOG</a>
ETTh	17420	7	<a href="https://github.com/zhouhaoyi/ETDataset">https://github.com/zhouhaoyi/ETDataset</a>
MuJoCo	10000	14	<a href="https://github.com/google-deepmind/dm_control">https://github.com/google-deepmind/dm_control</a>
Energy	19711	28	<a href="https://archive.ics.uci.edu/dataset">https://archive.ics.uci.edu/dataset</a>
fMRI	10000	50	<a href="https://www.fmrib.ox.ac.uk/datasets">https://www.fmrib.ox.ac.uk/datasets</a>

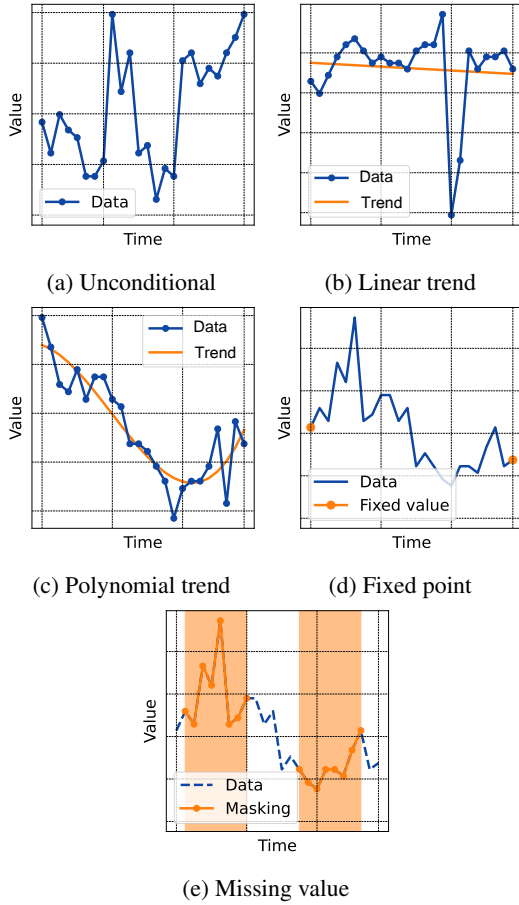


Figure 6: Illustration of time series generation situations on various conditions.

TS, unfortunately, we cannot achieve the performance of Diffusion-TS in their original paper.

Furthermore, for the conditional generations, we reimplement SSSD (Alcaraz and Strodtthoff 2023) using the official

GitHub <https://github.com/SSSD/sssd>. For the trend-guided synthesis, we treat the trend as conditional observations and train the SSSD model to match the total time-series data. We add the conditional embedding layers in their original model architectures.

## Experimental settings

### Model Architecture

We utilized Diffusion-TS (Yuan and Qiao 2024) as the based model, leveraging encoder-decoder transformer blocks. In this model, the encoder encodes the noisy sequence and the decoder consists of  $K$  decoder blocks, where each block is composed of a transformer block, a feed-forward network, and interpretable decomposition layers to reflect the trends and seasonality of time series data. Each interpretable layers consist of trend and seasonal synthesis layers.  $w_{(\cdot)}^{i,t}$  denotes the input of interpretable layers where  $i \in 1, \dots, K$  denotes the index of the corresponding decoder block at diffusion step  $t$ .

We synthesize trend components using polynomial regressor as follows:

$$V_{tr}^t = \sum_{i=1}^K (C \cdot \text{Linear}(w_{tr}^{i,t}) + X_{tr}^{i,t}), \quad (20)$$

where  $X_{tr}^{i,t}$  is the mean value of the output of the  $i^{th}$  decoder block,  $\cdot$  denotes the tensor multiplication and  $C = [1, c, \dots, c^p]$  for  $c = [0, 1, 2, \dots, \tau - 1]^T / \tau$ . We recover seasonal and error components using Fourier bases as follows:

$$A_{i,t}^{(k)} = |\mathcal{F}(w_{seas}^{i,t})_k|, \Phi_{i,t}^{(k)} = \phi(\mathcal{F}(w_{seas}^{i,t})_k), \quad (21)$$

$$\kappa_{i,t}^{(1)}, \dots, \kappa_{i,t}^{(K)} = \underset{k \in \{1, \dots, \lfloor \tau/2 \rfloor + 1\}}{\text{argTopK}} \{A_{i,t}^{(k)}\}, \quad (22)$$

$$S_{i,t} = \sum_{k=1}^K A_{i,t}^{\kappa_{i,t}^{(k)}} [\cos(2\pi f_{\kappa_{i,t}^{(k)}} \tau c + \Phi_{i,t}^{\kappa_{i,t}^{(k)}}) + \cos(2\pi \bar{f}_{\kappa_{i,t}^{(k)}} \tau c + \bar{\Phi}_{i,t}^{\kappa_{i,t}^{(k)}})], \quad (23)$$

---

**Algorithm 1:** Point-preserving Hybrid Sampler for TimeBridge

---

**Input:** Diffusion model  $D_\theta(\mathbf{x}_t)$ , score function  $\mathbf{s}(D_\theta, \mathbf{x}_{t_i}, t_i, \mathbf{x}_T, T)$  defined in Equation 9, diffusion steps  $\{0 = t_0 < \dots < t_\Gamma = T\}$ ; Condition  $\mathbf{y}$ , masking  $\mathbf{m}$ , step ratio  $s$

**Output:** Denoised output  $\mathbf{x}_0$

$\mathbf{x}_T \leftarrow$  Set the prior as the hard constraint condition  $\mathbf{y}$

**if** Imputation **then**  $\mathbf{x}_T \leftarrow$  Linear spline interpolation using Equation (12) with masking  $\mathbf{m}$

**for**  $i = \Gamma, \dots, 1$  **do**

**Sample**  $\varepsilon \sim \mathcal{N}(\mathbf{0}, \mathbf{I})$

$\tilde{t}_i \leftarrow t_i + s(t_{i-1} - t_i)$

$\mathbf{d}_{t_i} \leftarrow -\mathbf{f}(\mathbf{x}_{t_i}, t_i) + g^2(t_i)(\mathbf{s}(D_\theta, \mathbf{x}_{t_i}, t_i, \mathbf{x}_T, T) - \mathbf{h}(\mathbf{x}_{t_i}, t_i, \mathbf{x}_T, T))$

$\tilde{\mathbf{x}}_{t_i} \leftarrow \mathbf{x}_{t_i} + \mathbf{d}_{t_i} \odot \mathbf{m}(\tilde{t}_i - t_i) + g(t_i)\sqrt{\tilde{t}_i - t_i} \cdot \varepsilon \odot \mathbf{m}$

$\tilde{\mathbf{d}}_{t_i} \leftarrow -\mathbf{f}(\tilde{\mathbf{x}}_{t_i}, \tilde{t}_i) + g^2(\tilde{t}_i)(\frac{1}{2}\mathbf{s}(D_\theta, \tilde{\mathbf{x}}_{t_i}, \tilde{t}_i, \mathbf{x}_T, T) - \mathbf{h}(\tilde{\mathbf{x}}_{t_i}, \tilde{t}_i, \mathbf{x}_T, T))$

$\mathbf{x}_{t_{i-1}} \leftarrow \tilde{\mathbf{x}}_{t_i} + \tilde{\mathbf{d}}_{t_i} \odot \mathbf{m}(t_{i-1} - \tilde{t}_i)$

**if**  $i \neq 1$  **then**

$\mathbf{d}'_{t_i} \leftarrow -\mathbf{f}(\mathbf{x}_{t_{i-1}}, t_{i-1}) + g^2(t_{i-1})(\frac{1}{2}\mathbf{s}(D_\theta, \mathbf{x}_{t_{i-1}}, t_{i-1}, \mathbf{x}_T, T) - \mathbf{h}(\mathbf{x}_{t_{i-1}}, t_{i-1}, \mathbf{x}_T, T))$

$\mathbf{x}_{t_{i-1}} \leftarrow \tilde{\mathbf{x}}_{t_i} + \frac{1}{2}(\mathbf{d}'_{t_i} + \tilde{\mathbf{d}}_{t_i}) \odot \mathbf{m}(t_{i-1} - \tilde{t}_i)$

**end**

**end**

---

where  $\text{argTopK}$  is to get the top  $K$  amplitudes and  $K$  is a hyperparameter.  $A_{i,t}^{(k)}$  and  $\Phi_{i,t}^{(k)}$  are the phase, amplitude of the  $k$ -th frequency after the discrete Fourier transform  $\mathcal{F}$ , respectively.  $f_k$  represents the Fourier frequency of the corresponding index  $k$  and  $(\cdot)$  denotes  $(\cdot)$  of the corresponding conjugates.

### Diffusion Sampler

We make details of the point-preserving sampler and its usage in imputation as proposed in Algorithm 1. We further explain the details of our sampler for the unconditional situation in Algorithm 2.

For implementing the diffusion sampler, we modify the official code of DDBM (Zhou et al. 2024) in <https://github.com/alexzhou907/DDBM> as the backbone of our sampler.

### Hyperparameter Setups

For experimental setups, we follow the base setups of Yuan and Qiao (2024). Therefore, we try to use the minimal search space for determining only for diffusion scheduler  $\mathbf{x}_t = \alpha_t \mathbf{x}_0 + \sigma_t \varepsilon$ , where  $\alpha_t$  and  $\sigma_t$  are the functions of times.

As demonstrated in EDM (Karras et al. 2022), we can

---

**Algorithm 2:** Unconditional Hybrid Sampler for TimeBridge

---

**Input:** Diffusion model  $D_\theta(\mathbf{x}_t)$ , score function  $\mathbf{s}(D_\theta, \mathbf{x}_{t_i}, t_i, \mathbf{x}_T, T)$  defined in Equation 9, diffusion steps  $\{0 = t_0 < \dots < t_\Gamma = T\}$ , step ratio  $s$

**Output:** Denoised output  $\mathbf{x}_0$

**Sample**  $\mathbf{x}_T \sim$  prior using Equations (10) or (11)

**for**  $i = \Gamma, \dots, 1$  **do**

**Sample**  $\varepsilon \sim \mathcal{N}(\mathbf{0}, \mathbf{I})$

$\tilde{t}_i \leftarrow t_i + s(t_{i-1} - t_i)$

$\mathbf{d}_{t_i} \leftarrow -\mathbf{f}(\mathbf{x}_{t_i}, t_i) + g^2(t_i)(\mathbf{s}(D_\theta, \mathbf{x}_{t_i}, t_i, \mathbf{x}_T, T) - \mathbf{h}(\mathbf{x}_{t_i}, t_i, \mathbf{x}_T, T))$

$\tilde{\mathbf{x}}_{t_i} \leftarrow \mathbf{x}_{t_i} + \mathbf{d}_{t_i}(\tilde{t}_i - t_i) + g(t_i)\sqrt{\tilde{t}_i - t_i} \cdot \varepsilon$

$\tilde{\mathbf{d}}_{t_i} \leftarrow -\mathbf{f}(\tilde{\mathbf{x}}_{t_i}, \tilde{t}_i) + g^2(\tilde{t}_i)(\frac{1}{2}\mathbf{s}(D_\theta, \tilde{\mathbf{x}}_{t_i}, \tilde{t}_i, \mathbf{x}_T, T) - \mathbf{h}(\tilde{\mathbf{x}}_{t_i}, \tilde{t}_i, \mathbf{x}_T, T))$

$\mathbf{x}_{t_{i-1}} \leftarrow \tilde{\mathbf{x}}_{t_i} + \tilde{\mathbf{d}}_{t_i}(t_{i-1} - \tilde{t}_i)$

**if**  $i \neq 1$  **then**

$\mathbf{d}'_{t_i} \leftarrow -\mathbf{f}(\mathbf{x}_{t_{i-1}}, t_{i-1}) + g^2(t_{i-1})(\frac{1}{2}\mathbf{s}(D_\theta, \mathbf{x}_{t_{i-1}}, t_{i-1}, \mathbf{x}_T, T) - \mathbf{h}(\mathbf{x}_{t_{i-1}}, t_{i-1}, \mathbf{x}_T, T))$

$\mathbf{x}_{t_{i-1}} \leftarrow \tilde{\mathbf{x}}_{t_i} + \frac{1}{2}(\mathbf{d}'_{t_i} + \tilde{\mathbf{d}}_{t_i})(t_{i-1} - \tilde{t}_i)$

**end**

**end**

---

reparameterize  $\alpha_t$  and  $\sigma_t$  using  $\beta_{min}$  and  $\beta_d$  as follows:

$$\alpha_t = e^{-\frac{1}{4}\beta_d t^2 - \frac{1}{2}\beta_{min} t} \quad (24)$$

$$\sigma_t = e^{\frac{1}{2}\beta_d t^2 + \beta_{min} t} - 1, \quad (25)$$

With the aforementioned equations, we can adjust  $\alpha_t$  and  $\sigma_t$  based on  $\beta_{min}$  and  $\beta_d$ .

Furthermore, we can adjust the weight scheduler of  $w_t$  in Equation (13) with  $\sigma_{data}$  as in EDM (Karras et al. 2022) and DDBM (Zhou et al. 2024) as follows:

$$w_t = \frac{(\sigma_t^2 + \sigma_{data}^2)}{(\sigma_t \cdot \sigma_{data})^2}. \quad (26)$$

Note that EDM (Karras et al. 2022) and DDBM (Zhou et al. 2024) uses this  $\sigma_{data}$  in the reparametrization of  $F$ -matching in Equation (19) to calculate,  $c_{skip}, c_{out}, c_{in}, c_{noise}$ , but we exclude them since we use direct  $D$ -matching.

In the GP setups for the unconditional generation, we additionally search the kernel parameter  $\eta$ .

The summarized hyperparameters used for unconditional generation and conditional generation are demonstrated in Tables 9 and 10 for unconditional and conditional setting, respectively.

We unified the sampling settings with the second-order Heun sampler with 40 steps, which have 119 NFE. We use the churn ratio  $s = 0.33$  for stochastic sampling in Algorithms 1 and 2.

Table 9: Hyperparameters for unconditional generation.

Setup	Hyper-parameter	Search space	Sines	MuJoCo	ETTh	Stocks	Energy	fMRI
Base setup (Yuan and Qiao 2024)	Batch size	-	128	128	128	64	64	64
	Training steps	-	12000	14000	18000	10000	25000	15000
	Attention heads / head dim	-	4/16	4/16	4/16	4/16	4/24	4/24
	Layers of encoder / decoder	-	1/2	3/2	3/2	2/2	4/3	4/4
	Warmup Learning rate	-	0.008	0.008	0.008	0.008	0.008	0.008
	Optimizer	-	Adam	Adam	Adam	Adam	Adam	Adam
TimeBridge	$\beta_{min}$	{0.1, 0.2}	0.2	0.1	0.2	0.2	0.2	0.1
	$\beta_d$	{1, 2, 5, 10}	10	5	10	10	10	2
	$\sigma_{data}$	{0.05, 0.1, 0.5}	0.5	0.5	0.1	0.1	0.05	0.5
TimeBridge-GP	Kernel parameter $\eta$	{0.1, 0.3, 0.5, 1}	1	0.1	0.5	0.3	1	0.1

Table 10: Hyperparameters for conditional generation.

Method	Hyper-parameter	Search space	Trend & Imputation		
			Mujoco	ETTh	Energy
TimeBridge	$\beta_{min}$	{0.1}	0.1	0.1	0.1
	$\beta_d$	{0.2, 0.5, 1}	0.2	0.2	0.2
	$\sigma_{data}$	{0.05, 0.1, 0.5}	0.5	0.1	0.05 <sup>†</sup>

<sup>†</sup> We use 0.025 for the Energy dataset with Butterworth trend setting.

## Additional Experimental Results

### Generation with longer input

We conduct experiments to compare the long-term generation performance of our model with Diffusion-TS (Yuan and Qiao 2024), specifically over a time length of 64. The experimental results are shown in Table 11. We reproduced Diffusion-TS and achieved better performance compared to their results using a small number of selected data samples. Except for the Energy dataset, the proposed TimeBridge-GP outperformed in generation quality with an input length of 64.

### Generation with same NFE

Table 12 presents the experimental results for Diffusion-TS (Yuan and Qiao 2024) with the same NFE of 119 across most datasets. The results demonstrate that TimeBridge outperforms Diffusion-TS by using better priors for time series and the second-order sampler, compared to standard Gaussian priors.

### Predictive score

Predictive score (Yoon, Jarrett, and Van der Schaar 2019) measures the performance to predict the next step trained with synthetic data as a train-synthesis-and-test-real (TSTR) method. Table 13 illustrates the predictive score in the same experimental setting of Table 1. Similarly, Table 14 shows the predictive score of the same experiments as in Table 2.

### Ablation study

**VP and VE scheduler.** We perform experiments to compare the performance of the VP bridge and VE bridge for unconditional generation. The results, as shown in Table 15, indicate that the VP bridge consistently outperforms the VE

bridge in all measures. We hypothesize that the enlarging level of noise addition in VE might be harmful to time series generation.

**Importance of  $D$ -matching in time series.** To verify the effectiveness of  $D$ -matching in time series, we compare the performance of  $D$ -matching and  $F$ -matching methods for unconditional generation. The experimental results are shown in Table 16. It can be observed that  $D$ -matching yields better results in most metrics across the majority of datasets in our experiments.

**Importance of stochasticity.** We conduct experiments to compare the performance of the SDE solver with and without the stochasticity during sampling. By setting the step ratio to  $s = 0$ , we prevent noise from being added during sampling. The experimental results are presented in Table 17. The results show that the SDE solver performs better than the non-stochastic method. Note that TimeBridge-GP uses  $s = 0.33$ .

**Fourier-based loss.** Table 18 illustrates the strength of Fourier-based loss in diffusion sampling.

Table 11: Quality comparison of unconditional time series synthetic data with a length of 64.

Metric	Methods	Datasets			
		ETTh	Stocks	Energy	fMRI
Context-FID score (Lower is better)	Diffusion-TS (Yuan and Qiao 2024)	0.235±.011	0.948±.227	<b>0.067±.010</b>	3.662±.104
	<b>TimeBridge-GP</b>	<b>0.110±.009</b>	<b>0.693±.165</b>	0.072±.010	<b>0.527±.024</b>
Correlational score (Lower is better)	Diffusion-TS (Yuan and Qiao 2024)	0.061±.010	0.005±.005	<b>0.442±.077</b>	4.585±.068
	<b>TimeBridge-GP</b>	<b>0.038±.011</b>	<b>0.005±.003</b>	0.548±.102	<b>1.569±.028</b>
Discriminative score (Lower is better)	Diffusion-TS (Yuan and Qiao 2024)	0.078±.017	0.149±.035	<b>0.065±.011</b>	0.245±.234
	<b>TimeBridge-GP</b>	<b>0.045±.013</b>	<b>0.090±.018</b>	0.149±.005	<b>0.211±.184</b>
Predictive score (Lower is better)	Diffusion-TS (Yuan and Qiao 2024)	0.115±.002	0.038±.001	<b>0.249±.010</b>	0.103±.000
	<b>TimeBridge-GP</b>	<b>0.114±.005</b>	<b>0.038±.000</b>	0.250±.001	<b>0.100±.000</b>

Table 12: Comparison of generation performance with same NFE of 119.

Metric	Methods	Synthetic datasets		Real datasets			
		Sines	MuJoCo	ETTh	Stocks	Energy	fMRI
Context-FID score (Lower is better)	Diffusion-TS (Yuan and Qiao 2024)	0.014±.001	0.033±.006	0.244±.012	0.252±.014	0.126±.026	0.149±.009
	<b>TimeBridge-GP</b>	<b>0.006±.001</b>	<b>0.016±.002</b>	<b>0.067±.007</b>	<b>0.054±.009</b>	<b>0.064±.007</b>	<b>0.096±.008</b>
Correlational score (Lower is better)	Diffusion-TS (Yuan and Qiao 2024)	<b>0.015±.002</b>	0.194±.023	0.071±.011	0.021±.004	<b>0.878±.144</b>	1.079±.024
	<b>TimeBridge-GP</b>	0.018±.003	<b>0.173±.025</b>	<b>0.034±.004</b>	<b>0.008±.008</b>	0.902±.218	<b>0.839±.018</b>
Discriminative score (Lower is better)	Diffusion-TS (Yuan and Qiao 2024)	0.043±.014	0.040±.008	0.103±.006	0.130±.009	<b>0.143±.008</b>	0.156±.016
	<b>TimeBridge-GP</b>	<b>0.002±.002</b>	<b>0.006±.003</b>	<b>0.052±.002</b>	<b>0.049±.014</b>	0.165±.009	<b>0.082±.033</b>
Predictive score (Lower is better)	Diffusion-TS (Yuan and Qiao 2024)	0.095±.000	<b>0.008±.001</b>	0.125±.005	0.038±.000	<b>0.251±.000</b>	<b>0.099±.000</b>
	<b>TimeBridge-GP</b>	<b>0.093±.000</b>	0.009±.001	<b>0.121±.006</b>	<b>0.037±.000</b>	<b>0.251±.000</b>	0.100±.000

Table 13: Predictive score unconditional time series synthetic data. The best results are in **bold** and the second best are underlined.

Metric	Methods	Synthetic datasets		Real datasets			
		Sines	MuJoCo	ETTh	Stocks	Energy	fMRI
Predictive score (Lower is better)	TimeVAE (Desai et al. 2021) <sup>†</sup>	<b>0.093±.000</b>	0.012±.002	0.126±.004	0.039±.000	0.292±.000	0.113±.003
	TimeGAN (Yoon, Jarrett, and Van der Schaar 2019) <sup>†</sup>	<b>0.093±.019</b>	0.025±.003	0.124±.001	<u>0.038±.001</u>	0.273±.004	0.126±.002
	Cot-GAN (Xu et al. 2020) <sup>†</sup>	<u>0.100±.000</u>	0.068±.009	0.129±.000	0.047±.001	<u>0.259±.000</u>	0.185±.003
	Diffwave (Kong et al. 2021) <sup>†</sup>	<b>0.093±.000</b>	0.013±.000	0.130±.001	0.047±.000	<b>0.251±.000</b>	0.101±.000
	Diffusion-TS (Yuan and Qiao 2024)	<b>0.093±.000</b>	<b>0.007±.001</b>	<u>0.123±.003</u>	<b>0.037±.000</b>	<b>0.251±.000</b>	<b>0.100±.000</b>
	<b>TimeBridge-GP</b>	<b>0.093±.000</b>	<u>0.009±.001</u>	<b>0.121±.006</b>	<b>0.037±.000</b>	<b>0.251±.000</b>	<b>0.100±.000</b>

The baseline experimental results (denoted by †) are adopted from (Yuan and Qiao 2024). We re-implement Diffusion-TS with their official code.

Table 14: Quality comparison of trend-conditioned time series synthetic data.

Metric	Methods	ETTh			Energy		
		Linear	Polynomial	Butterworth	Linear	Polynomial	Butterworth
Predictive score	Trend Baseline	0.1208±.0035	0.1200±.0016	0.1210±.0030	0.3684±.0085	0.4065±.0362	0.3744±.0413
	SSSD (Alcaraz and Strodthoff 2023)	0.1228±.0041	0.1206±.0036	0.1214±.0047	0.2498±.0005	0.2501±.0004	0.2498±.0004
	Diffusion-TS (Yuan and Qiao 2024)	0.1204±.0055	0.1200±.0059	0.1197±.0060	0.2503±.0003	<b>0.2500±.0005</b>	<b>0.2495±.0007</b>
	<b>TimeBridge-GP</b>	<b>0.1195±.0062</b>	<b>0.1196±.0061</b>	<b>0.1196±.0060</b>	<b>0.2501±.0002</b>	<b>0.2500±.0005</b>	0.2502±.0003

Table 15: Quality comparison of unconditional time series with VP and VE scheduler.

Metric	Methods	Synthetic datasets		Real datasets			
		Sines	MuJoCo	ETTh	Stocks	Energy	fMRI
Context-FID score (Lower is better)	TimeBridge-GP-VP	<b>0.006±.001</b>	<b>0.016±.002</b>	<b>0.067±.007</b>	<b>0.054±.009</b>	<b>0.064±.007</b>	<b>0.096±.008</b>
	TimeBridge-GP-VE	0.011±.002	0.031±.004	0.256±.028	0.130±.028	0.184±.0.03	0.102±.009
Correlational score (Lower is better)	TimeBridge-GP-VP	<b>0.018±.003</b>	<b>0.173±.025</b>	<b>0.034±.004</b>	<b>0.008±.008</b>	<b>0.902±.218</b>	<b>0.839±.018</b>
	TimeBridge-GP-VE	0.027±.003	0.190±.010	0.060±.011	0.065±.006	1.115±.160	0.895±.021
Discriminative score (Lower is better)	TimeBridge-GP-VP	<b>0.002±.002</b>	<b>0.006±.003</b>	<b>0.052±.002</b>	<b>0.049±.014</b>	<b>0.165±.009</b>	<b>0.082±.033</b>
	TimeBridge-GP-VE	0.017±.009	0.026±.011	0.089±.009	0.095±.000	0.236±.012	0.109±.013
Predictive score (Lower is better)	TimeBridge-GP-VP	<b>0.093±.000</b>	<b>0.009±.001</b>	<b>0.121±.006</b>	<b>0.037±.000</b>	<b>0.251±.000</b>	<b>0.100±.000</b>
	TimeBridge-GP-VE	<b>0.093±.000</b>	0.010±.001	0.122±.005	0.038±.000	<b>0.251±.000</b>	<b>0.100±.000</b>

Table 16: Quality comparison of unconditional time series with  $D$ -matching and  $F$ -matching.

Metric	Methods	Synthetic datasets		Real datasets			
		Sines	MuJoCo	ETTh	Stocks	Energy	fMRI
Context-FID score (Lower is better)	TimeBridge-D	<b>0.008±.001</b>	<b>0.018±.002</b>	<b>0.069±.004</b>	0.079±.023	<b>0.082±.007</b>	<b>0.097±.008</b>
	TimeBridge-F	0.011±.002	0.023±.003	0.093±.010	<b>0.060±.013</b>	0.101±.006	0.104±.008
	TimeBridge-GP-D	<b>0.006±.001</b>	<b>0.016±.002</b>	<b>0.067±.007</b>	<b>0.054±.009</b>	<b>0.064±.007</b>	<b>0.096±.008</b>
	TimeBridge-GP-F	0.019±.004	0.019±.004	0.087±.010	0.068±.014	0.081±.006	0.106±.008
Correlational score (Lower is better)	TimeBridge-D	0.024±.001	<b>0.179±.011</b>	<b>0.035±.005</b>	<b>0.009±.009</b>	1.064±.167	<b>0.914±.028</b>
	TimeBridge-F	<b>0.016±.002</b>	0.184±.017	0.037±.004	0.011±.007	<b>0.904±.134</b>	1.076±.048
	TimeBridge-GP-D	<b>0.018±.003</b>	<b>0.173±.025</b>	<b>0.034±.004</b>	0.008±.008	0.902±.218	<b>0.839±.018</b>
	TimeBridge-GP-F	0.033±.009	0.181±.028	0.038±.006	<b>0.007±.005</b>	<b>0.885±.246</b>	1.104±.031
Discriminative score (Lower is better)	TimeBridge-D	<b>0.012±.003</b>	<b>0.007±.008</b>	<b>0.052±.004</b>	<b>0.052±.021</b>	<b>0.167±.003</b>	0.077±.010
	TimeBridge-F	0.031±.013	0.016±.011	0.053±.017	0.070±.011	0.167±.006	<b>0.045±.026</b>
	TimeBridge-GP-D	<b>0.002±.002</b>	<b>0.006±.003</b>	<b>0.052±.002</b>	<b>0.049±.014</b>	<b>0.165±.009</b>	0.082±.033
	TimeBridge-GP-F	0.006±.005	0.019±.010	0.052±.012	0.065±.017	0.170±.007	<b>0.036±.038</b>
Predictive score (Lower is better)	TimeBridge-D	<b>0.093±.000</b>	0.009±.001	<b>0.121±.006</b>	<b>0.037±.000</b>	<b>0.251±.000</b>	<b>0.100±.000</b>
	TimeBridge-F	0.095±.000	<b>0.008±.001</b>	<b>0.121±.006</b>	<b>0.037±.000</b>	<b>0.251±.000</b>	<b>0.100±.000</b>
	TimeBridge-GP-D	<b>0.093±.000</b>	0.009±.001	<b>0.121±.006</b>	<b>0.037±.000</b>	<b>0.251±.000</b>	<b>0.100±.000</b>
	TimeBridge-GP-F	<b>0.093±.000</b>	<b>0.008±.001</b>	<b>0.121±.006</b>	<b>0.037±.000</b>	<b>0.251±.000</b>	<b>0.100±.000</b>

Table 17: Quality comparison of unconditional time series with sampling step ratio  $s$ .

Metric	Methods	Synthetic datasets		Real datasets			
		Sines	MuJoCo	ETTh	Stocks	Energy	fMRI
Context-FID score (Lower is better)	TimeBridge-GP	<b>0.006±.001</b>	<b>0.016±.002</b>	<b>0.067±.007</b>	<b>0.054±.009</b>	<b>0.064±.007</b>	<b>0.096±.008</b>
	TimeBridge-GP- $s = 0$	1.956±.149	4.878±.571	6.582±.615	3.531±.263	3.439±.268	10.491±1.066
Correlational score (Lower is better)	TimeBridge-GP	<b>0.018±.003</b>	<b>0.173±.025</b>	<b>0.034±.004</b>	<b>0.008±.008</b>	<b>0.902±.218</b>	<b>0.839±.018</b>
	TimeBridge-GP- $s = 0$	0.431±.005	0.618±.044	0.441±.010	0.157±.007	3.741±.138	5.235±.091
Discriminative score (Lower is better)	TimeBridge-GP	<b>0.002±.002</b>	<b>0.006±.003</b>	<b>0.052±.002</b>	<b>0.049±.014</b>	<b>0.165±.009</b>	<b>0.082±.033</b>
	TimeBridge-GP- $s = 0$	0.323±.041	0.445±.018	0.423±.048	0.374±.026	0.499±.000	0.497±.008
Predictive score (Lower is better)	TimeBridge-GP	<b>0.093±.000</b>	<b>0.009±.001</b>	<b>0.121±.006</b>	<b>0.037±.000</b>	<b>0.251±.000</b>	<b>0.100±.000</b>
	TimeBridge-GP- $s = 0$	0.095±.001	0.018±.002	0.148±.005	0.050±.006	0.255±.002	0.102±.000

Table 18: Quality comparison of unconditional time series without Fourier.

Metric	Methods	Synthetic datasets		Real datasets			
		Sines	MuJoCo	ETTh	Stocks	Energy	fMRI
Context-FID score (Lower is better)	TimeBridge-GP	<b>0.006±.001</b>	<b>0.016±.002</b>	<b>0.067±.007</b>	<b>0.054±.009</b>	<b>0.064±.007</b>	<b>0.096±.008</b>
	w/o Fourier	0.007±.002	0.018±.003	0.087±.010	0.085±.020	0.093±.011	0.097±.008
Correlational score (Lower is better)	TimeBridge-GP	0.018±.003	0.173±.025	<b>0.034±.004</b>	<b>0.008±.008</b>	<b>0.902±.218</b>	<b>0.839±.018</b>
	w/o Fourier	0.018±.004	<b>0.172±.022</b>	0.036±.005	0.010±.008	0.942±.198	0.848±.023
Discriminative score (Lower is better)	TimeBridge-GP	<b>0.002±.002</b>	<b>0.006±.003</b>	<b>0.052±.002</b>	0.049±.014	<b>0.165±.009</b>	<b>0.082±.033</b>
	w/o Fourier	0.004±.004	0.010±.006	0.060±.004	<b>0.035±.027</b>	0.216±.007	0.096±.006

## Visualization

**Visualization of distribution properties.** In addition to visualization of the synthetic data on t-SNE Figure 3, we visualize the synthetic data of TimeBridge using PCA kernel and kernel density estimation in Figures 7 and 8, respectively. More visualization results on baseline methods can be found in the Appendix of Diffusion-TS (Yuan and Qiao 2024).

**Sampling paths.** In Figure 9, we additionally provide the sampling path from prior to data samples (left-to-right), as shown in Figure 4a. Here, we visualize the priors with GP, linear trend, polynomial trend, and Butterworth trend.

**Imputation.** In Figure 10, we additionally provide the sampling path from linear spline of masked values as prior to data samples (left-to-right), as shown in Figure 4b.

In Figure 11, we further visualize the results of imputation, as shown in Figure 5.

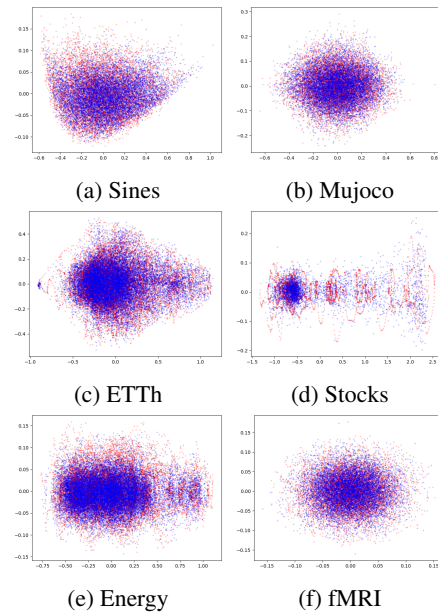


Figure 7: Visualization on PCA. Red and blue indicate original and synthetic data, respectively.

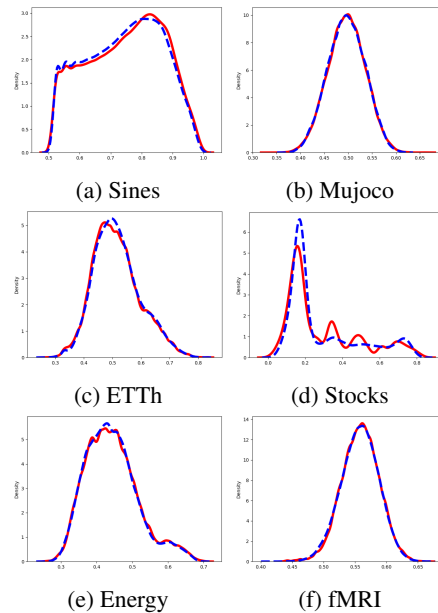
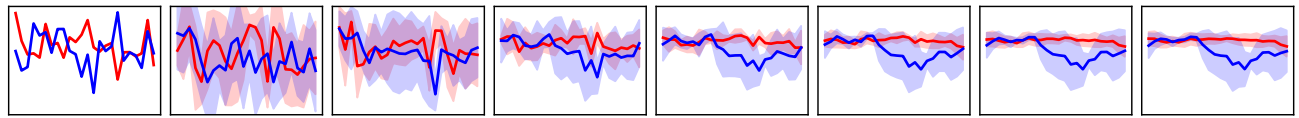
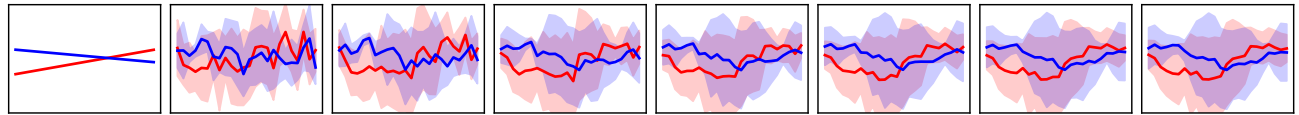
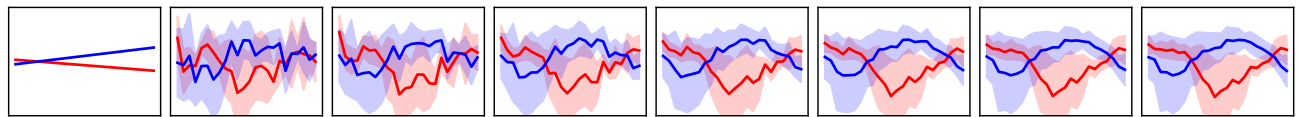
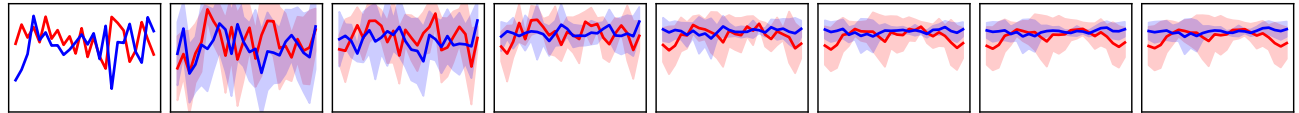


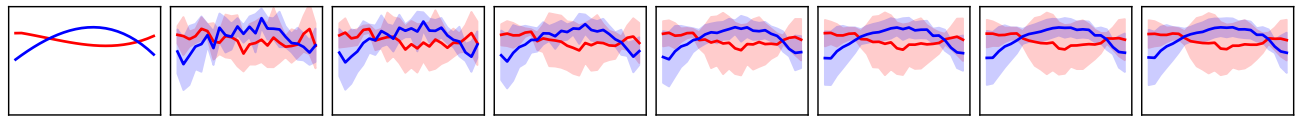
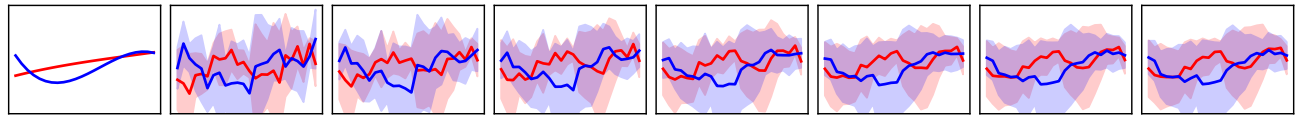
Figure 8: Visualization of the kernel density estimation. Red and blue indicate original and synthetic data, respectively.



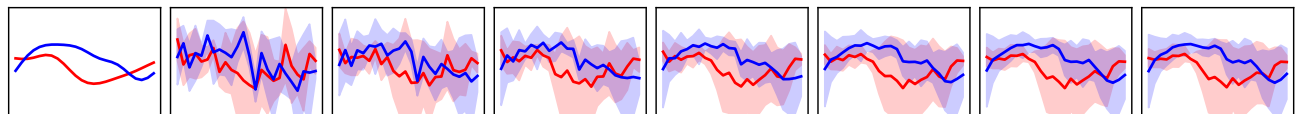
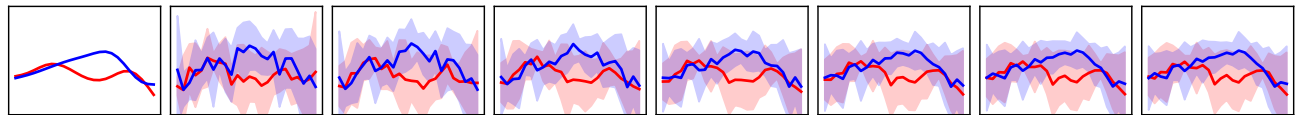
(a) Unconditional (GP)



(b) Linear trend



(c) Polynomial trend



(d) Butterworth trend

Figure 9: Sampling path from (Left) the prior to (Right) the data samples with diverse prior settings on the ETTh dataset.

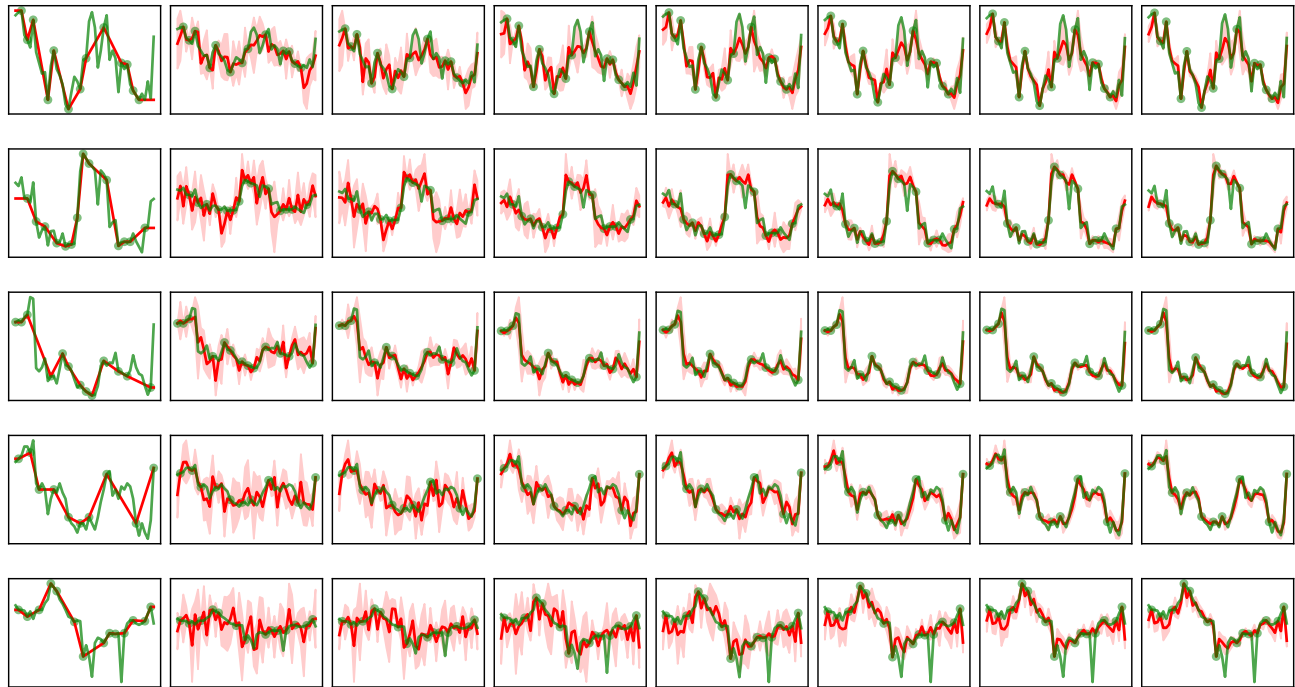


Figure 10: Sampling path from the prior (Left) to the imputation (Right) of TimeBridge (red) using point-preserving sampling based on observed values (dots) of the truth (green).

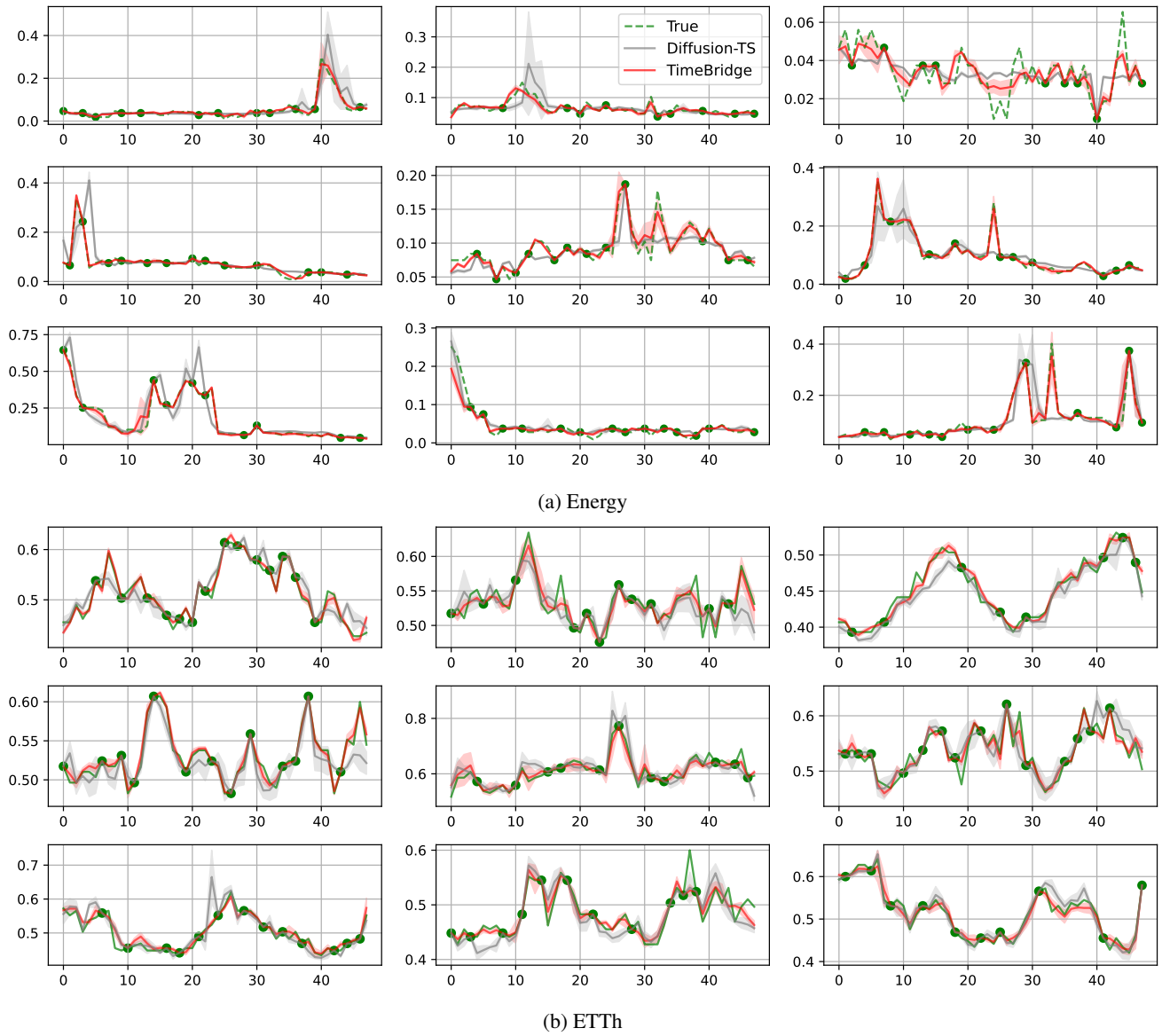


Figure 11: Visualization of imputation on (Top) Energy and (Bottom) ETTh dataset. The green dotted lines denote the true and the green circles denote the observed value. Diffusion-TS and TimeBridge are visualized with grey and red along with their interval.